Received: 5 August 2022 | Revised: 18 December 2023 | Accepted: 8 January 2024

DOI: 10.1111/mec.17272

ORIGINAL ARTICLE

MOLECULAR ECOLOGY WILEY

Genetic structure, UV-vision, wing coloration and size coincide with colour polymorphism in *Fabriciana adippe* butterflies

Daniela Polic[1] | Yeşerin Yıldırım[1] | Sami Merilaita[2] | Markus Franzén[1] | Anders Forsman[1]

[1]Department of Biology and Environmental Science, Linnaeus University, Kalmar, Sweden

[2]Department of Biology, University of Turku, Turku, Finland

Correspondence
Daniela Polic, Department of Biology and Environmental Science, Linnaeus University, Kalmar, Sweden.
Email: daniela.polic@lnu.se

Present address
Yeşerin Yıldırım, Department of Ecology and Genetics, Uppsala University, Uppsala, Sweden

Funding information
Entomologiska Föreningen Stockholm; Linnéuniversitetet; Erasmus+ Mobility Program; Svenska Forskningsrådet Formas, Grant/Award Number: 2018-02846; The Carl Trygger Foundation

Handling Editor: Jeremy B Yoder

Abstract

Colour polymorphisms have long served as model systems in evolutionary studies and continue to inform about processes involved in the origin and dynamics of biodiversity. Modern sequencing tools allow for evaluating whether phenotypic differences between morphs reflect genetic differentiation rather than developmental plasticity, and for investigating whether polymorphisms represent intermediate stages of diversification towards speciation. We investigated phenotypic and genetic differentiation between two colour morphs of the butterfly *Fabriciana adippe* using a combination of ddRAD-sequencing and comparisons of body size, colour patterns and optical properties of bright wing spots. The silvery-spotted *adippe* form had larger and darker wings and reflected UV light, while the yellow *cleodoxa* form displayed more green scales and reflected very little UV, showcasing that they constitute distinct and alternative integrated phenotypes. Genomic analyses revealed genetic structuring according to source population, and to colour morph, suggesting that the phenotypic differentiation reflects evolutionary modifications. We report 17 outlier loci associated with colour morph, including *ultraviolet-sensitive visual pigment* (*UVRh1*), which is associated with intraspecific communication and mate choice in butterflies. Together with the demonstration that the wings of the *adippe* (but essentially not the *cleodoxa*) morph reflect UV light, that UV reflectance is higher in females than males and that morphs differ in wing size, this suggests that these colour morphs might represent genetically integrated phenotypes, possibly adapted to different microhabitats. We propose that non-random mating might contribute to the differentiation and maintenance of the polymorphism.

KEYWORDS
alternative integrated phenotypes, assortative mating, colour polymorphism, ddRAD-sequencing, evolution, genetic correlation

1 | INTRODUCTION

Colour polymorphisms provide eye-catching examples of biological diversity and have been of long-standing interest to evolutionary biologists and ecologists, as they offer powerful model systems for studying and understanding natural selection, evolution of local adaptations, phenotypic integration, as well as mechanisms influencing the dynamics and maintenance of genetic and phenotypic variation within populations (Bond, 2007; Fisher, 1939; Ford, 1945; Forsman et al., 2008, 2020; McKinnon & Pierotti, 2010; Sapir et al., 2021; Schwander & Leimar, 2011; Stuart-Fox et al., 2021; Takahashi & Hori, 2008; True, 2003). Theory and empirical evidence further suggest that colour polymorphism may enhance the ecological success of populations and species (Forsman, 2016; Forsman et al., 2008; Forsman & Wennersten, 2016; Wennersten & Forsman, 2012; Yildirim et al., 2018) and serve as a driver for evolutionary diversification and speciation (Forsman, 2016; Forsman et al., 2008; Gray & McKinnon, 2007; McLean & Stuart-Fox, 2014).

There is ample evidence that differences in animal colour patterns can directly contribute to variation in performance and lifetime reproductive success (i.e. relative fitness) of individuals, for example, by influencing susceptibility to predators, intraspecific signalling for mate choice, capacity for temperature regulation, protection from UV-radiation and resistance to desiccation and abrasion (Huey & Kingsolver, 1989; Ruxton et al., 2004; Wellenreuther et al., 2014). Because animal colour patterns have multifarious functions, a change in one component may induce selection that modifies the combination of size, shape, colour and position of other pattern components, and this may contribute to the integration and differentiation of multiple colour pattern elements (Fisher, 1930; Nijhout, 1991; Polic et al., 2023; Tsai et al., 2020). In many species, colour patterns are associated with body size, behaviours or other phenotypic traits (Ahnesjö & Forsman, 2003; Forsman et al., 2008; McKinnon & Pierotti, 2010; True, 2003). Such associations between traits, also known as phenotypic integration, may represent evolutionary responses to correlational selection that favours certain combinations of trait values over other combinations, that is, when the selective benefit of a given trait value depends on the value of another trait (Brodie, 1992; Dingemanse et al., 2020; Fisher, 1939; Forsman & Appelqvist, 1998; Lande & Arnold, 1983; Svensson et al., 2021). Their underpinnings include (but are not limited to) linkage disequilibrium, pleiotropy, close linkage and shared developmental pathways (Andersson, 2001; Falconer & Mackay, 1996; Fruciano et al., 2016; Svensson et al., 2021; True, 2003); however, they can also be a result of phenotypic plasticity (Schlichting & Wund, 2014).

Once established, alternative morphs and trait-value combinations may be maintained by the evolution of assortative mating, which can prevent the disruption and break-up of co-adapted gene complexes and favourable trait-value combinations (Jiang et al., 2013; Lancaster et al., 2014; Tamin & Doligez, 2022). As colour patterns play an important role for visual signalling and mate choice in many species, assortative mating according to colour morph or selection against offspring from mixed parents might contribute to continued differentiation between colour morphs (Gray & McKinnon, 2007). This can ultimately lead to reproductive isolation with respect to colour morph, as previously reported in visually oriented animals such as butterflies, birds and fishes (e.g. Kronforst et al., 2006; Roulin, 2004; Whitney et al., 2018).

Despite the considerable and growing scientific interest that colour polymorphisms attract (see figure 1 in Forsman, 2016), there remain open questions awaiting to be answered. For example, our understanding of the drivers, evolutionary dynamics and consequences of colour polymorphisms is potentially complicated by that discrete variations in colour patterns do not always have an underlying genetic basis; they can also result from developmental plasticity (polyphenism) when a single genotype produces alternative phenotypes in response to some environmental cue (Pfennig et al., 2010; Schwander & Leimar, 2011; Whitman & Agrawal, 2009). Similarly, associations between different colour pattern elements, and associations of colour pattern with other traits need not reflect underlying genetic correlations, they can also result from plasticity integration (Pfennig et al., 2010; Pigliucci & Preston, 2004; Whitman & Agrawal, 2009). The effects of selection and reproductive isolation, the evolutionary modifications and divergence of integrated phenotypes, and the consequences for population performance all depend on whether colour morphs have a genetic underpinning (Garner et al., 2020; Hughes et al., 2008; Lande, 1998; Wennersten & Forsman, 2012). To identify the proximate mechanisms controlling the expression of colour polymorphisms and associated traits is therefore key to understand their evolutionary dynamics (e.g. Caillaud & Losey, 2010; Rankin & Stuart-Fox, 2015; San-Jose & Fitze, 2013). Many previous studies on the genetics of colour polymorphism in terrestrial animals have focussed on differences between morphs along environmental or geographic gradients (e.g. Brusa et al., 2013; Ghisbain et al., 2020; Hegna et al., 2015; Hoekstra et al., 2004; McLean et al., 2015). There are also several examples of sympatric polymorphisms in different types of organisms, where the genetic or regulatory basis of morph determination has been identified (Brien et al., 2023; Chamberlain et al., 2009; Fisher, 1930; Funk et al., 2021; Gratten et al., 2007; Hoekstra & Nachman, 2003; Jeong et al., 2022; Joron et al., 2011; Kunte et al., 2014; Lamichhaney et al., 2016; Nabours, 1929; Rankin et al., 2016; Shakya et al., 2021; VanKuren et al., 2022; Westerman, Letchinger, et al., 2018; Westerman, VanKuren, et al., 2018; Winter et al., 2021), but demonstrations of overall genetic differentiation between colour morphs within populations are relatively scarce (but see Russo et al., 1994).

The recent developments in DNA sequencing tools have opened new possibilities to further the understanding of the above issues, and more. For instance, high-throughput technologies such as double-digested restriction-site-associated DNA sequencing (ddRADseq) can generate thousands of single nucleotide polymorphism (SNP) loci randomly distributed across both coding (functional) and non-coding regions of the genome (Andrews et al., 2016). This makes ddRADseq a powerful tool to analyse genetic diversity and structure, genetic associations with phenotypic traits such as

colour morphs, and to identify genomic regions potentially under selection (Andrews et al., 2016; Peterson et al., 2012).

The butterfly species *Fabriciana adippe* is well-suited for examining whether sympatric colour morphs are genetically manifested, whether colour morphs are phenotypically and genetically correlated with other traits, and whether the dynamics and maintenance of the polymorphism is influenced by selective processes such as assortative mating (Lank, 2002; Pérez i de Lanuza et al., 2013). Throughout the distribution area, the High Brown Fritillary occurs in several discrete colour morphs, two of which are present in our study area in Sweden (Figure 1), the nominate form *F. adippe* f. *adippe* with silvery, iridescent mother-of-pearl like spots on the ventral hindwings, and *F. adippe* f. *cleodoxa*, which instead has light yellow spots (Eliasson et al., 2005; Tolman & Lewington, 2012). In butterflies, reflective silvery patterns may enhance camouflage and thereby protect against predators, and may be involved in intraspecific signalling during mate choice, particularly in habitats with complex light conditions such as forest habitats (Wilts et al., 2013), but this has not yet been confirmed for *F. adippe*. To our knowledge, the colour polymorphism in *F. adippe* has not been well characterized, potential multivariate phenotypic integration within and differentiation between the *adippe* and the *cleodoxa* morph has not been evaluated, and the genetic background of the colour polymorphism and associated traits has not been previously investigated in this species.

In the present study of colour polymorphism in *F. adippe*, we integrate phenotypic and genetic sequencing data for butterflies collected from one mainland and two insular natural populations in Sweden. Specifically, we (i) characterize the wing colour pattern polymorphism and quantify phenotypic integration and differentiation by examining whether the *adippe* and *cleodoxa* colour morphs are phenotypically and genetically correlated with other traits (viz. forewing length, degree of melanism, the amount of green and orange wing scales, and optical properties (i.e. reflectance of UV and longer wavelengths (390–700 nm)) of the bright spots). As colour polymorphisms are often associated with other phenotypic (e.g. morphological) traits in many organisms (see above), we expect some covariation between morphological characteristics in the respective colour morphs. If phenotypic traits covary with genetic structuring, this might suggest that these trait combinations have a genetic underpinning, rather than stemming from plasticity responses. We also (ii) assess whether the colour polymorphism is accompanied by an overall genetic differentiation between sympatric morphs across populations. A genetic differentiation between morphs that is accompanied by other distinct trait values might suggest evolutionary modifications, possibly owing to selection. Lastly, we (iii) performed outlier analyses to identify loci putatively under selection and discuss environmental factors or processes contributing to evolutionary differentiation and maintenance of the colour polymorphism.

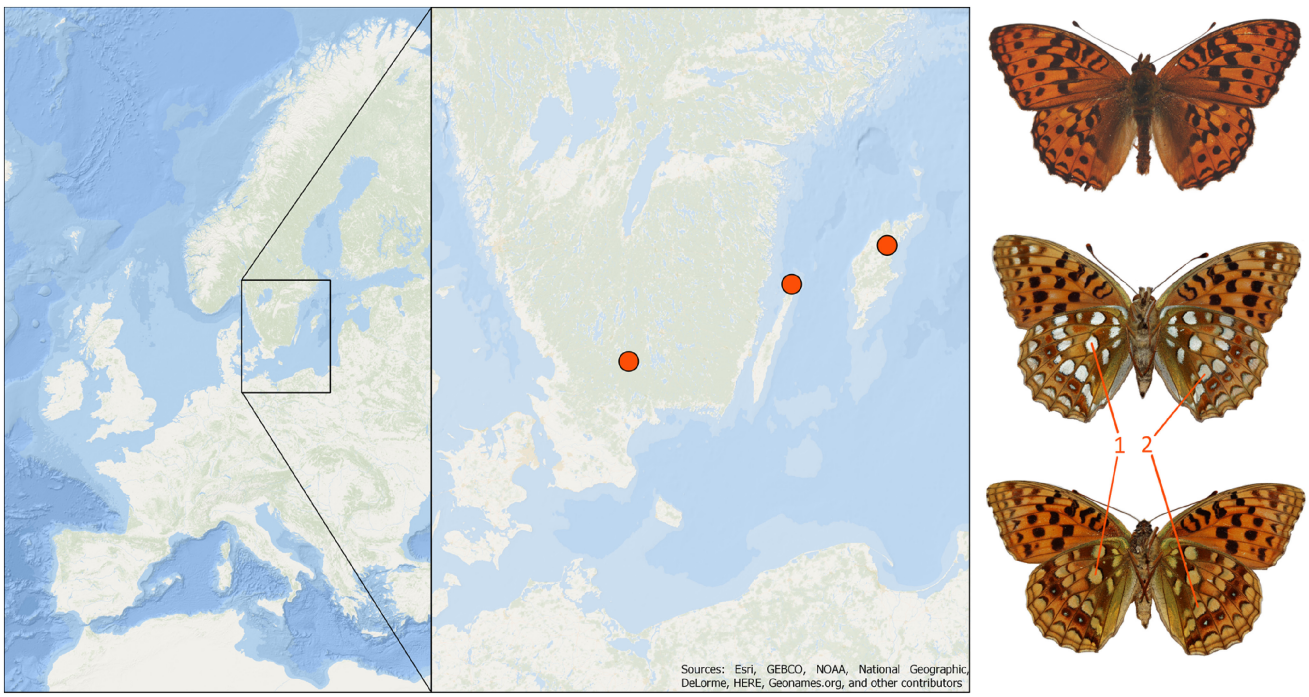

FIGURE 1 Map of study area. The red spots indicate the three studied Swedish populations in Småland, and the islands Öland and Gotland (from left to right). The pictures on the right side show the dorsal side of *Fabriciana adippe*, the ventral side of *F. adippe* f. *adippe* with silvery spots on the ventral hindwings, and *F. adippe* f. *cleodoxa* with yellow spots (from top to bottom). The red lines and numbers indicate the location of the two spots on the ventral side of the hind wing, where the reflection probe was used to quantify optical properties (spectral reflectance) of the silvery spots of the *adippe* morph and the corresponding yellow spots in the *cleodoxa* morph.

2 | MATERIALS AND METHODS

2.1 | Study species

Fabriciana adippe occurs in large parts of the Palearctic and is widely distributed in Scandinavia, ranging as far north as central Sweden (Eliasson et al., 2005, Tolman & Lewington, 2012). While both colour morphs can occur in the same area, the nominate form *F. adippe* f. *adippe* is progressively replaced by the yellow form *F. adippe* f. *cleodoxa* southwards through central Europe to the Balkans and Greece, where the latter morph is dominating (Tolman & Lewington, 2012). In their northern distribution area, *F. adippe* butterflies breed in bracken (*Pteridium aquilinum*) dominated habitats within woodland landscapes, grass and *P. aquilinum* mosaics, as well as in glades, clear-cuttings and meadows in forest dominated landscapes (Eliasson et al., 2005; Warren, 1995). The univoltine species usually lays its eggs, which constitute the overwintering life stage, on or in close proximity to its larval food plants, viz. *Viola* species (Eliasson et al., 2005).

2.2 | Study area and data collection

We collected butterflies belonging to both colour morphs *F. adippe* f. *adippe* and *F. adippe* f. *cleodoxa* from three Swedish populations, viz. Småland, and the islands Öland and Gotland in summer 2017 (see map in Figure 1). From this collection, we selected 18 (14 *adippe*, 4 *cleodoxa*), 39 (23 *adippe*, 16 *cleodoxa*) and 29 (25 *adippe*, 4 *cleodoxa*) individuals from Småland, Öland, and Gotland, respectively, such that both sexes were represented in each population and colour morph (Table 1). Butterflies were either directly transferred to 95–99% ethanol or dried and kept at −20°C in the laboratory at the Department of Biology and Environmental Science, Linnaeus University in Kalmar until DNA extraction.

2.3 | Quantifying body size and wing colour patterns

To obtain data on body size and wing colour patterns, each butterfly was photographed in front of standard white paper with a Nikon D3000 camera using an 18–55 mm lens without flash, with the left ventral fore- and hindwing and the right dorsal fore- and hindwing (i.e. four parts) facing the camera, together with a ruler (Polic et al., 2023). The camera was placed in a fixed position, that is, 34 cm from the wings. Each picture was taken with the same settings (focal length 35 mm, ISO 400, shutter speed 1/200 s, aperture f/4.5) and light conditions, in the butterfly laboratory at Institut de Biologia Evolutiva in Barcelona, Spain. We used the software GIMP 2 to measure the wing size and colours. Using the *ruler* tool, we measured forewing (and hindwing) length as the straight linear distance from the apex of the forewing (and hindwing) to its base. In each of the 4 wing parts (left ventral fore- and hindwing, right dorsal fore- and hindwing), we used the "select by colour" tool to select and measure the number of pixels of a certain colour, viz. "light brown" (#92580f), "dark brown" (#4a3822), "black" (#0a0907), "light orange" (#c88d00), "dark orange" (#a55400), "white" (#f2f4e7), "grey" (#b5b498), "yellow" (#c5a035), "light green" (#7b7f20), and "dark green" (#565d17) with a threshold of 15 (Polic et al., 2023). Then, we calculated the percentage of each colour in each wing part. Dark brown and black pixels were added up and defined as the degree of melanism in each wing, which is also referred to as the degree of darkness in the text. The added percentages of dark and light green in the ventral hindwing (only present in this wing part) were defined as the variable "green". Hereafter, "orange" refers to the percentage of orange in all 4 wing parts. For the statistical analyses of phenotypic integration and composite phenotypic differentiation between colour morphs, we used data on wing size (forewing length, hindwing length) and colour patterns of the wings (forewing melanism, hindwing melanism, green and orange).

For the statistical analyses used to evaluate phenotypic associations with the genetic structure (described below), we used dorsal melanism as a measure of darkness and forewing length as a measure of wing size. Dorsal melanism was used since butterflies expose their dorsal wings when sun basking to increase their body temperature (Clench, 1966; Kingsolver, 1985). Forewing length is commonly used as a proxy for body size in butterflies and is highly correlated with wing area, which is important for temperature regulation (Kingsolver & Koehl, 1985; Stuhldreher et al., 2014) and flight capacity (Berwaerts et al., 2002; Kalarus et al., 2013; Skórka et al., 2013).

TABLE 1 Number of individuals from each colour morph, sex and population used in this study.

Colour morph	Småland	Öland	Gotland	Wing size [mm]	Melanism [%]	Green [%]	Orange [%]
F. adippe f. *adippe*	14	23	25	26.24 (±1.69)	34 (±9)	16 (±11)	8 (±5)
female	3	12	10	26.97 (±2.09)	33 (±10)	12 (±5)	6 (±4)
male	11	11	15	25.76 (±1.18)	36 (±8)	19 (±12)	9 (±5)
F. adippe f. *cleodoxa*	4	16	4	25.38 (±1.82)	29 (±8)	22 (±13)	8 (±4)
female	2	4	2	26.65 (±2.07)	30 (±10)	22 (±16)	9 (±4)
male	2	12	2	24.74 (±1.34)	29 (±6)	22 (±12)	7 (±4)

Note: The right side of the table shows the mean wing size (measured as forewing length) in mm, the mean summed percentage of dark brown and black scales in the dorsal wings ("Melanism"), the mean percentage of green scales in the ventral hindwings ("Green"), and the mean percentage of orange scales in all four parts of the wings ("Orange"). Standard deviations are shown in brackets.

Individuals were classified according to colour morph based on the presence of the silvery or yellow spots, respectively, on the ventral hindwings (Figure 1, Table S1).

2.4 | Quantifying optical properties of the bright wing spots

For a straightforward approach of comparing the optical properties of the bright wing spots between individuals, we chose two of the spots (silvery or yellow respectively) on the ventral side of the right hind wing (Figure 1), and used a JAZ spectrophotometer with a JAZ-PX light source (both Ocean Optics, Dunedin, FL) and a small-tip reflection probe (Avantes, the Netherlands) for the measurement of spectral reflectance of the spots. All measurements were conducted relative to a white, diffuse reflectance standard. Because the measured spots of the *adippe* morph were iridescent, their reflectance spectrum and intensity vary with the angle of light and viewing. We therefore used five individuals for an initial approximation of the angle of the probe, yielding highest maximal reflectance of the measured spots. Based on these measurements, we used a fixed 75° angle to the plane of the wing for the final measurements. For each measurement, we adjusted the rotational (horizontal) angle by starting at a perpendicular angle to the wing base and the longitudinal axis of the body, and then slightly rotated the measured wing clockwise and anti-clockwise, to find the angle that yielded the highest reflectance. This was repeated three times for each measured spot. In the analysis of reflectance, we used the highest value of the three repeated measurements for each spot (Table S1).

Specifically, we aimed at assessing the relative intensity of the UV component in the bright spots. To our knowledge, neither the spectral sensitivity of *UVRh1* nor the maximum wavelength sensitivity for *F. adippe* has been directly tested. Studies of other butterflies report that the UV-sensitive photoreceptor (dark purple) encoded by the *UVRh1* gene covers the band from around 325 to 385 nm, with a peak in sensitivity around 355 nm, and that the visual sensitivity interval extends to around 650 nm, albeit with some variation between species and sexes (Briscoe et al., 2010; Bybee et al., 2012; Finkbeiner & Briscoe, 2021; Ogawa et al., 2013). Although *F. adippe* may differ from other species, we set the range of UV sensitivity of *UVRh1* from 325 to 385, and the maximum wavelength sensitivity to 700 nm. For each individual and spot, we then estimated the summed reflectance within the UV (325–385 nm) and within longer wavelengths (hereafter LW, 390–700 nm), and then calculated the ratio of UV/LW reflectance to estimate the salience of the UV component. Estimates of measurement repeatability from one-way ANOVAs (Lessells & Boag, 1987; Nakagawa & Schielzeth, 2010) based on data from two measurements (spot 1 and 2) of 22 individuals showed that reflectance was quantified with high accuracy (>85%) for all three variables (UV: $F_{21,22}=16.99$, $p<.001$, Repeatability = 88.9%; LW: $F_{21,22}=12.05$, $p<.001$, Repeatability = 88.8%; UV/LW: $F_{21,22}=42.97$, $p<.001$, Repeatability = 95.5%).

2.5 | Statistical evaluation of phenotypic integration and composite phenotypic differentiation between colour morphs

To evaluate and compare phenotypic integration between morphs, we first analysed pairwise associations between the two wing size measures and the four wing colour pattern variables (see above) using Spearman correlation analysis. This was done separately for the two morphs. Next, to evaluate whether the integration between different phenotypic traits is parallel or independent in the two colour morphs, we tested whether pairs of phenotypic traits that were highly positively or weakly negatively correlated in one morph were also highly positively or weakly negatively correlated in the other morph, using a correlation analysis. Finally, to evaluate whether the strength of phenotypic integration was equal or different in the two morphs, we tested for a difference in the absolute value of the 15 pairwise trait correlations using a paired *t*-test.

To evaluate whether overall composite phenotypic variation differed between colour morphs, after controlling for variation due to source population and sex, we first used a principal component analysis (PCA, a dimension reducing approach) to describe the total phenotypic variation in the six original phenotypic traits in two dimensions (principal component axes, PCA1 and PCA2). This was done for all three populations pooled, with procedure PRINCOMP in SAS 9.4 (Windows version 1.0.19041), and the results visualized in a biplot, to evaluate whether composite phenotypic variation overlapped or differed between morphs. Next, to formally evaluate whether the composite phenotypic variation differed markedly according to colour morph after statistically accounting for variation due to population and sex, we performed a multivariate analysis of variance (MANOVA, implemented with procedure GLM in SAS 9.4) using PC1 and PC2 as dependent variables, and population, sex and colour morph as explanatory factors. To enable visualization of the average composite differentiation, we estimated least squares means and associated 95% confidence limits of PC1 and PC2 for the two morphs, from the MANOVA.

In addition to the multivariate analyses, we tested for differentiation between colour morphs by performing separate 3-way analyses of variance for the different traits. These analyses were implemented with procedure GLM in SAS 9.4. Colour morph, source population and sex were treated as discrete explanatory variables, and forewing length, hindwing length, dorsal melanism, green, and orange were treated as response variables (the two latter variables were square root transformed to achieve normal distribution). First, we tested for both main and interaction effects of colour morph, source population and sex on the phenotypic traits. Non-significant interaction effects were removed stepwise from the models.

To identify sources of variation in the optical properties of wing spots, differences in summed reflectance between colour morphs, sexes and populations were evaluated using mixed model ANOVAs, implemented with procedure MIXED in SAS 9.4 (Windows version 1.0.19041), with individual identity included as a random factor to account for repeated measures within individuals.

2.6 | Library preparation and ddRAD-sequencing

Genomic DNA (gDNA) was extracted by grinding thorax tissue with stainless steel beads (Next Advance, USA) in a bullet blender, and E.Z.N.A.® Genomic DNA Isolation Kit (OMEGA Bio-Tek, USA) was used for further processing. We used agarose gel electrophoresis to estimate the quality of gDNA. The DNA samples with relatively low quality were subjected to whole genome amplification using REPLI-g Mini Kit (Qiagen) to obtain sufficient gDNA in quantity and quality prior to double-digested restriction site-associated DNA sequencing (ddRADseq).

Double-digested restriction site-associated DNA sequencing (ddRADseq) libraries were prepared following the protocol in Peterson et al. (2012) and Lee et al. (2018) with some modifications. For details, see Library preparation and ddRAD-sequencing in Appendix S1. We used the *process_radtags* unit in Stacks 2.2 (Catchen et al., 2011, 2013) to de-multiplex the raw data and for quality control, and the *integrated* approach (Catchen et al., 2011, 2013; Paris et al., 2017) for assembly of ddRADtag loci and SNP calling. The recently published *Fabriciana adippe* genome (GenBank assembly GCA_905404265.1) was used for aligning the catalogue. For details, see Quality control and data trimming in Appendix S1. The final catalogue used for downstream analyses contained 6401 loci.

2.7 | Wolbachia testing to evaluate the potential role of parasite genetic contamination

The sequences obtained after *populations* in Stacks were mapped to the *Wolbachia pipientis* genome (GenBank: NZ_JQAM01000001) using Geneious 11.1.05 (Biomatters) to evaluate the risk of contamination by the bacterial parasite *Wolbachia*, which could influence the outcome of the population genetic analyses (Werren et al., 2008). As none of the catalogue loci could be mapped to *Wolbachia*, we concluded that *Wolbachia* contamination would not affect the outcome of our analyses to a significant extent.

2.8 | Analysing genetic structure

We used multiple approaches with different algorithms to investigate the genetic structure among colour morphs and populations for the purpose of obtaining a more comprehensive picture. The following analyses were utilized and are explained in detail in Analysing genetic structure in Appendix S1. We obtained estimates of the fixation index F_{ST} (Weir & Cockerham, 1984) in Arlequin 3.5 (Excoffier et al., 2005), we used Principal Component Analysis (PCA) in R 3.6.1 (R Core Team, 2020), and PERMANOVA+ add-in (Gorley & Clarke, 2008) in PRIMER-R 7 (Gorley & Clarke, 2006) for Permutation Analysis of Variance (PERMANOVA) (McArdle & Anderson, 2001), PERMDISP (Anderson, 2006), and Canonical Analysis of Principal coordinates (CAP) (Anderson & Willis, 2003). We assessed phylogenetic relationships between individuals using the maximum likelihood (ML) tree inference in IQ-TREE 2.1.2 (Nguyen et al., 2015) and used Interactive Tree Of Life (iTOL) 6 for visualization (Letunic & Bork, 2019).

2.9 | Evaluating associations of genetic structure with population, sex, colour morph and phenotypic traits

Since we found that discrete colour morphs also differed significantly in other traits (see Section 3.1), we tested for associations of the genetic structure with phenotypic variables (forewing length, dorsal melanism, the percentage of green on the ventral hindwing and the total percentage of orange in the wings), colour morph (i.e. *adippe* with silvery-white spots or *cleodoxa* with yellow spots), sex and source population by utilizing a distance-based redundancy analysis (db-RDA), which constitutes a constrained version of PCA (Legendre & Anderson, 1999). The same distance matrix as for PCA was converted into a Manhattan dissimilarity matrix and used for principal coordinates analysis (PCoA). The *capscale* function in the R package VEGAN 2.5 (Oksanen et al., 2019) was used to build db-RDA models, which assessed the variables contributing the most to the PCoA ordination. The function *anova* determined the statistical significance of the explanatory variables using 999 permutations. We also performed separate db-RDA for each population (Småland, Öland, Gotland) to assess associations of the genetic structure with the above-mentioned variables on a higher geographic resolution, and to explore whether the pattern of overall genetic differentiation between colour morphs was consistent across populations. When building the db-RDA models, we calculated the variance inflation factor (VIF) for each predictor variable, and excluded variables with a VIF > 10 from the model, as such high values might indicate a problematic level of collinearity with other variables (James et al., 2013). Since our phenotypic variables are dimensionally heterogeneous, we standardized them using *z*-scoring; for each variable, we subtracted the mean value from the observed value and then divided this by the standard deviation.

2.10 | Outlier analysis to identify genes associated with colour morph

To identify genes putatively under selection associated with colour morph identity, we searched for outliers correlated with colour morph using two different approaches: BayeScEnv 1.1 (de Villemereuil & Gaggiotti, 2015), which is an F_{ST}-based genome-scan method, and a coalescent approach, Fdist in Arlequin (Excoffier & Lischer, 2010). For details, see Outlier analysis in Appendix S1. Manhattan plots were generated in R 3.6.1 (R Core Team, 2020) using the *p* values from these analyses. To assess the potential functional roles of the outlier loci, we interrogated the outlier sequences against coding sequences from all available Lepidopteran

reference genomes in Lepbase 4 (Challi et al., 2016) using the BLAST interface (Priyam et al., 2019). We calculated allele frequencies in each population for the outlier loci that mapped to coding regions. We also checked the protein-coding genes residing between the two SNPs flanking each outlier locus in Ensembl genome browser 110 (genome release GCA_905404265.1), and annotation was conducted with Ensembl Genebuild method by Lohse et al. (2022). Inbreeding coefficient (F_{IS}) and violations of Hardy–Weinberg equilibrium (HWE) at these loci were calculated in the *populations* unit in Stacks.

We also searched for outlier loci associated with sex using BayeScEnv by assigning −1 and 1 as environmental variables to females and males respectively.

3 | RESULTS

3.1 | Phenotypic integration and differentiation between colour morphs

The analyses of phenotypic integration based on pairwise correlations between different traits showed that forewing size and hindwing size were positively correlated in both colour morphs, that the amount of green was negatively correlated with hindwing melanism in the *adippe* morph, and that forewing melanism tended to decrease with forewing size in the *adippe* morph (Table S2). The analyses of pairwise correlations further showed that phenotypic integration between the different wing size and colour pattern traits was not parallel in the two colour morphs ($r=0.47$, $n=15$, $p=.08$), and that trait correlations were stronger overall in *cleodoxa* than in *adippe* (paired *t*-test based on absolute correlation coefficients, $t=2.43$, $n=15$, $p=.029$, Table S2).

The quantification of composite phenotypic variation as described by the first two principal component scores (Prin1 and Prin2) accounted for 51% of the total variance in the two wing size traits and the four colour pattern traits (Table S3). Composite phenotypic variation, as quantified by Prin1 and Prin2, differed significantly between colour morphs, sexes and populations (MANOVA, colour morph: Wilks' lambda=0.84, $F_{2,71}=6.61$, $p=.0023$; sex: Wilks' lambda=0.51, $F_{2,71}=18.10$, $p<.0001$; population: Wilks' lambda=0.84, $F_{4142}=4.06$, $p=.0038$, Figure 2). On average, individuals belonging to the *adippe* morph had larger wings, a higher degree of melanism (darker coloration) and a lower proportion of green scales on the underside of the hindwing compared with *cleodoxa*, whereas individuals belonging to the *cleodoxa* morph had paler (less melanic) hindwings, a higher proportion of green scales on the underside of the hindwings and a higher percentage of orange summed across all four wing parts compared with *adippe* (Figure S1). The results from separate univariate analyses of variation in the different traits according to colour morph, sex and population (reported in Table S4) support that colour morphs differed in darkness (degree of melanism) and the proportion of green scales on the underside of the hindwings.

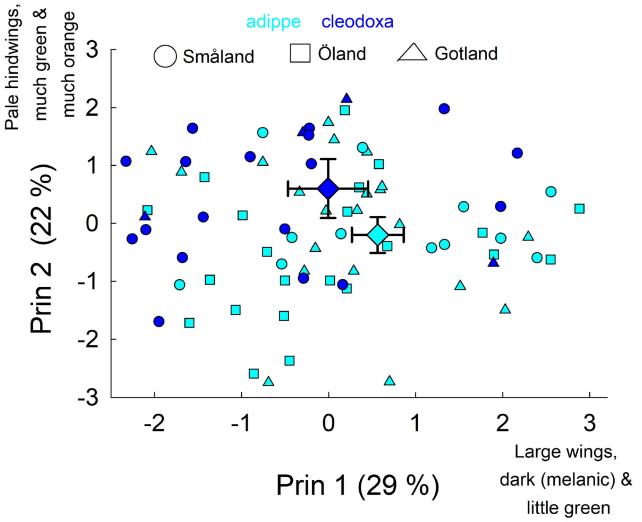

FIGURE 2 Biplot illustrating the composite phenotypic differentiation between *Fabriciana adippe* butterflies resulting from PCA, according to colour morph (*adippe/cleodoxa*) indicated by symbol colours and source population (Småland, Öland and Gotland) indicated by symbol shapes. Large positive values on Prin1 indicate large wings, a higher degree of melanism (darker coloration), and a low proportion of green scales on the underside of the hindwing. Large positive values on Prin2 indicate that hindwings are pale (less melanic), a high proportion of green scales on the underside of the hindwings, and a high percentage of orange summed across all four wing parts. Large diamonds show least squares means (±95% confidence limits) of PC1 and PC2 scores for each colour morph obtained from a MANOVA (see Tables S2 and S3). Differences between colour morphs are statistically significant (Prin1: $F_{1,72}=4.56$, $p=.036$; Prin2: $F_{1,72}=7.72$, $p=.007$, see text for further details).

3.2 | Optical properties of the bright wing spots

The optical properties (spectral reflectance) of the two measured wing spots varied according to colour morph, sex and population (Figure 3). Overall, reflectance in the UV interval was about 15 times higher in *adippe* than in *cleodoxa* individuals when controlling for the variation owing to sex and population reported in Table 2 (comparison of Least-squares means ± SE: *adippe* 473.44±31.29; *cleodoxa* 16.52±36.76, $t_{14}=9.46$, $p<.001$). UV reflectance was about two times higher overall in *adippe* females than in males (Table 2, Figure 3). Reflectance in the longer wavelengths visible to butterflies (LW, 390–700 nm) differed between colour morphs ($F_{1,17}=33.89$, $p<.001$), but not between sexes ($F_{1,17}=1.02$, $p=.33$) or populations ($F_{2,17}=0.86$, $p=.43$). The relative intensity of the UV component ranged from 0 to 0.14 among individuals and was overall significantly higher in *adippe* than in *cleodoxa* when controlling for the variation owing to sex and population reported in Table 2 (Least-squares means ± SE: *adippe* 0.087±0.0032; *cleodoxa* 0.006±0.0038, $t_{14}=16.37$, $p<.001$, Figure 3).

None of the *cleodoxa* individuals from Öland and Gotland reflected in the UV-spectrum. By contrast, all six (four females and two males) *cleodoxa* individuals from Småland showed weak

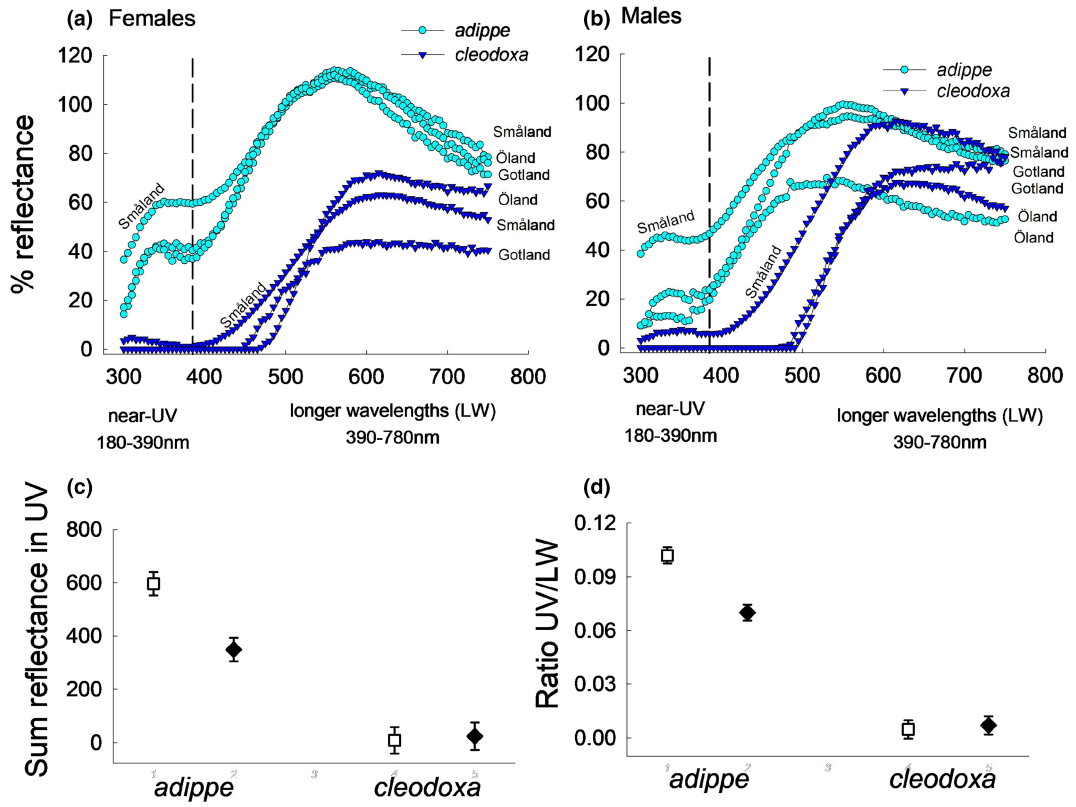

FIGURE 3 Comparisons of reflectance in *Fabriciana adippe* f. *adippe* and f. *cleodoxa* (a) females and (b) males from three different source populations. Reflectance was quantified for two of the silvery iridescent spots in the *adippe* morph and two corresponding yellow spots in the *cleodoxa* morph (Figure 1). Bottom panels show (c) sum of reflectance in the UV (325–385 nm) and (d) ratio of the summed reflectance in the UV and longer wavelength (LW, 390–700 nm) spectra for *adippe* and *cleodoxa* females (open squares) and males (black diamonds). Values represent least-squares means ± SE estimated from the mixed model ANOVAs presented in Table 2.

			UV (325–385 nm)		Ratio UV/LW	
Source of variation	Num DF	Den DF	*F*	*p*	*F*	*p*
Morph	1	14	89.58	<.0001	268.12	<.0001
Sex	1	14	6.08	.0272	9.93	.0071
Population	2	14	5.99	.0132	20.37	<.0001
Morph*Sex	1	14	7.82	.0143	13.16	.0027
Morph*Population	2	14	2.98	.0834	4.24	.0363

Note: Reflectance was quantified for two silvery iridescent spots on the ventral hind wings in the *adippe* morph and the corresponding yellow spots in *cleodoxa* morph in males and females from three populations. Results from mixed model ANOVAs, implemented with procedure MIXED in SAS, treating individual identity as a random factor. The covariance parameter estimate associated with the random effect of individual identity pointed to individual variation in UV reflectance also within populations, sexes, and colour morphs (UV: $Z = 1.47$, $p = .070$; ratio UV/LW: $Z = 1.42$, $p = .078$).

TABLE 2 Sources of variation in spectral reflectance in the UV (summed over the 325–385 nm interval) and in the ratio of summed reflectance in the UV and longer wavelengths (LW, 390–700 nm) in *Fabriciana adippe* butterflies.

reflectance in the UV, but the magnitude of the UV reflectance and the relative intensity of the UV component was two to seven times higher in the *adippe* morph (Figure 3). The above variation among populations was paralleled in the *adippe* morph, with individuals from Småland reflecting more in the UV band compared with individuals from Öland and Gotland, in both males and females (Figure 3).

According to results from the outlier analyses (for details, see Section 3.6 below, and Table 3), the differences between populations in reflectance in the UV band coincided with a molecular difference between populations in the frequency of the *UVRh1* receptor genotypes (alleles T and A). In the entire sample, nearly all (17 of 18) individuals from Småland belonged to the T/T genotype, whereas nearly half (25 of 69) of the individuals from Gotland and

TABLE 3 The position of outlier loci, the adjacent SNPs at both 5′ and 3′ ends, and the protein-coding genes residing at these loci. Lepbase 4 (Challi et al., 2016).

SNP ID	Chromo-some number	BP	Coding_region[a]	Description	5′-end adjacent SNP (position – bp)	3′-end adjacent SNP (position – bp)	Protein-coding gene(s) between the adjacent SNPs[b]
436607	3	6170906	*Heliconius erato demophoon* (evm. model. Herato1108.399)	Not_available	6044915	6284751	ENSFADG00005005498.1, ENSFADG00005003750.1, ENSFADG00005021706.1, ENSFADG00005021992.1, ENSFADG00005022030.1, ENSFADG00005022064.1
466356	5	5174267	No hits found		5154512	5301315	ENSFADG00005001776, ENSFADG00005006832, ENSFADG00005002435 (proprotein convertase subtilisin/kexin type 4), ENSFADG00005002113, ENSFADG00005004469, ENSFADG00005006846 (RNA polymerase II subunit B), ENSFADG00005005903, ENSFADG0000502118, ENSFADG00005008776 (zinc and ring finger 4), ENSFADG00005006268 (pecanex 4)
483706	6	8844269	No hits found		8791143	8908538	ENSFADG00005000956, ENSFADG00005022125 (SANT and BTB domain regulator of CSR), ENSFADG00005021194 (RAD23 homologue A, nucleotide excision repair protein a), ENSFADG00005005265 (kelch like family member 36), ENSFADG00005021707, ENSFADG00005021330, ENSFADG00005022026, ENSFADG00005021429 (cAMP responsive element binding protein 1), ENSFADG00005022146 (elongator acetyltransferase complex subunit 4), ENSFADG00005000624
507979	8	3465275	*Amyelois transitella* (cds XM_013334625.1)	Peptidyl-prolyl cis-trans isomerase-like 2 (PPIL2)	3401883	3468234	ENSFADG00005006931.1, ENSFADG00005006550.1, ENSFADG00005002860.1, ENSFADG00005022047.1
519968	9	224848	No hits found		69386	236834	No protein-coding sequences.
558020	11	15218769	No hits found		15173518	15218886	ENSFADG00005016405.1, ENSFADG00005013915.1, ENSFADG00005011904.1, ENSFADG00005010719.1
436607	12	899942	No hits found		823534	1303289	ENSFADG00005015024.1 (alkaline phosphatase, biomineralization associated), ENSFADG00005014709.1, ENSFADG00005013579.1, ENSFADG00005013519.1, ENSFADG00005012205.1, ENSFADG00005010876.1 (ephrin A5), ENSFADG00005008485.1 (RAB21, member RAS oncogene family), ENSFADG00005007801.1 (RAN binding protein 3 like), ENSFADG00005007103.1 (ABI family, member 3 (NESH) binding protein b), ENSFADG00005006943.1
561022	12	1504232	*Pieris napi* (cds_ PIENAPT00000012009)	Hypothetical protein	1477969	1504285	ENSFADG00005011790.1 (aggrecan a), ENSFADG00005009011.1 (eukaryotic translation initiation factor 5B)

(Continues)

TABLE 3 (Continued)

SNP ID	Chromo-some number	BP	Coding_region[a]	Description	5′-end adjacent SNP (position – bp)	3′-end adjacent SNP (position – bp)	Protein-coding gene(s) between the adjacent SNPs[b]
574013	13	1815873	No hits found		1815780	1874387	ENSFADG00005014737.1 (RIO kinase 2), ENSFADG00005014530.1 (sorbitol dehydrogenase), ENSFADG00005014231.1, ENSFADG00005010956.1, ENSFADG00005010223.1
612986	16	5894112	No hits found		5893707	5979856	ENSFADG00005003671 (G protein pathway suppressor 1), ENSFADG00005000245, ENSFADG00005006380, ENSFADG00005006380, ENSFADG00005001922, ENSFADG00005000168
613857	16	7004019	*Heliconius Melpomene* (cds HMEL010962-RA)	Ultraviolet-sensitive visual pigment (UVRh1)	6969358	7131340	ENSFADG00005010835.1, ENSFADG00005009223.1, ENSFADG00005009082.1, ENSFADG00005007897.1, ENSFADG00005007559.1, ENSFADG00005006520.1, ENSFADG00005003988.1, ENSFADG00005003474.1, ENSFADG00005000819.1 (modulator of smoothened), ENSFADG00005000704.1, ENSFADG00005000145.1, ENSFADG00005000130.1, ENSFADG00005020994.1, ENSFADG00005021073.1, ENSFADG00005021310.1
647580	19	4412368	No hits found		4236778	4592061	ENSFADG00005008711.1, ENSFADG00005008562.1, ENSFADG00005007569.1 (potassium two pore domain channel subfamily K member 9), ENSFADG00005006908.1, ENSFADG00005006119.1 (glutamyl-prolyl-tRNA synthetase 1), ENSFADG00005005806.1, ENSFADG00005005739.1, ENSFADG00005005240.1 (ST6 (alpha-N-acetyl-neuraminyl-2,3-beta-galactosyl-1,3)-N-acetylgalactosaminide alpha-2,6-sialyltransferase 1, tandem duplicate 1), ENSFADG00005005161.1 (coiled-coil-helix-coiled-coil-helix domain containing 4), ENSFADG00005005091.1, ENSFADG00005004695.1 (adaptor related protein complex 3 subunit sigma 1), ENSFADG00005003892.1, ENSFADG00005003878.1, ENSFADG00005003608.1, ENSFADG00005003164.1, ENSFADG00005001877.1 (ribosomal RNA processing 36), ENSFADG00005000066.1 (dihydrolipoamide S-succinyltransferase), ENSFADG00005009149.1 (phosphatidylcholine transfer protein), ENSFADG00005020796.1 (SUMO specific peptidase 6)

TABLE 3 (Continued)

SNP ID	Chromo-some number	BP	Coding_region[a]	Description	5′-end adjacent SNP (position – bp)	3′-end adjacent SNP (position – bp)	Protein-coding gene(s) between the adjacent SNPs[b]
655184	19	14024672	*Heliconius Melpomene* (cds HMEL008189g1.t1)	Ribosome-releasing factor 2 (RRF2)	13900644	14024819	ENSFADG00005019355.1, ENSFADG00005018981.1, ENSFADG00005018474.1, ENSFADG00005018168.1 (5′-3′ exoribonuclease 2), ENSFADG00005017794.1
664030	20	9930676	No hits found		9923879	9930984	ENSFADG00005006197.1
665736	20	12068284	*Heliconius erato lativitta* (cds HEL_014503-RA)	Peptidyl-tRNA hydrolase 2	12011681	12166459	ENSFADG00005020128.1 (telomerase RNA component interacting RNase), ENSFADG00005020094.1, ENSFADG00005020091.1, ENSFADG00005020072.1, ENSFADG00005020065.1, ENSFADG00005019980.1, ENSFADG00005019956.1, ENSFADG00005019946.1, ENSFADG00005019870.1, ENSFADG00005019799.1 (opioid related nociceptin receptor 1), ENSFADG00005019775.1, ENSFADG00005019739.1 (coiled-coil domain containing 63), ENSFADG00005019685.1
715006	25	11065451	No hits found		10817338	11079371	ENSFADG00005020526.1, ENSFADG00005020522.1, ENSFADG00005020502.1, ENSFADG00005020493.1, ENSFADG00005020414.1 (slit guidance ligand)
732229	28	53381	No hits found		18494	78145	ENSFADG00005015995.1, ENSFADG00005015941.1, ENSFADG00005015867.1, ENSFADG00005015784.1, ENSFADG00005015102.1 (histidine triad nucleotide binding protein 2), ENSFADG00005014932.1, ENSFADG00005014597.1 (neutral cholesterol ester hydrolase 1)

[a]The outlier sequences were interrogated against coding sequences from all available Lepidopteran reference genomes in Lepbase 4 (Challi et al., 2016) using the BLAST interface.

[b]The protein-coding genes were searched in Ensembl website (genome release GCA_905404265.1).

Öland belonged to the A/A genotype (Tables 4 and 5). In the sample ($n=22$) used to quantify reflectance, only the four male *adippe* individuals from Öland and Gotland, with relatively low UV reflectance (Figure 3), belonged to the A/A genotype, whereas all others, including the six individuals from Småland (both males and females and regardless of colour morph) belonged to the T/T genotype.

TABLE 4 Allele frequencies of the gene *ultraviolet-sensitive visual pigment* (left) in *F. adippe* populations.

Ultraviolet-sensitive visual pigment				
Population	**Allele**	**Overall**	***Adippe***	***Cleodoxa***
Gotland	T	0.52	0.44	1
	A	0.48	0.56	0
Öland	T	0.61	0.40	1
	A	0.39	0.60	0
Småland	T	0.94	0.93	1
	A	0.06	0.07	0

3.3 | Genetic structure

All populations were significantly differentiated from each other according to F_{ST} values (Gotland – Öland: 0.023, Gotland – Småland: 0.018, Öland – Småland: 0.013, $p<.001$ for all comparisons). The F_{ST} values for all pairwise comparisons between colour morphs within and among populations ranged up to 0.037. Despite the low F_{ST} values, the majority of comparisons showed significant differentiations ($p<.05$, Figure 4). The genetic differentiation between colour morphs within populations was highly significant in Öland ($F_{ST}=0.012$, $p<.001$) and Småland ($F_{ST}=0.023$, $p=.012$), but was not statistically significant in Gotland ($F_{ST}=0.000$, $p=.99$). Notice that the sample size for Gotland-*cleodoxa* was the lowest ($n=4$), which likely decreased the power of the permutation tests. However, population sample size can be significantly reduced, as long as a large enough number of bi-allelic genetic markers is used (>1000), which is the case in the present study (Willing et al., 2012).

According to the results generated by PCA, individuals belonging to the same colour morph largely clustered together (Figure 4b), but the structuring according to source population was manifested

TABLE 5 Genotype information for the gene *ultraviolet-sensitive visual pigment* (*UVRh1*) in *F. adippe* populations.

			***UVRh1* genotypes (*adippe/cleodoxa*)**			
Population	**No. of *adippe* morphs**	**No. of *cleodoxa* morphs**	**T/T**	**A/A**	**T/A**	**Missing data (*adippe/cleodoxa*)**
Gotland	25	5	15 (11/4)	14 (14/0)	0	1 (0/1)
Öland	23	16	18 (7/11)	11 (11/0)	3 (3/0)	7 (2/5)
Småland	14	4	17 (13/4)	1 (1/0)	0	0
Total	62	25	50 (31/19)	26 (26/0)	3 (3/0)	8 (2/6)

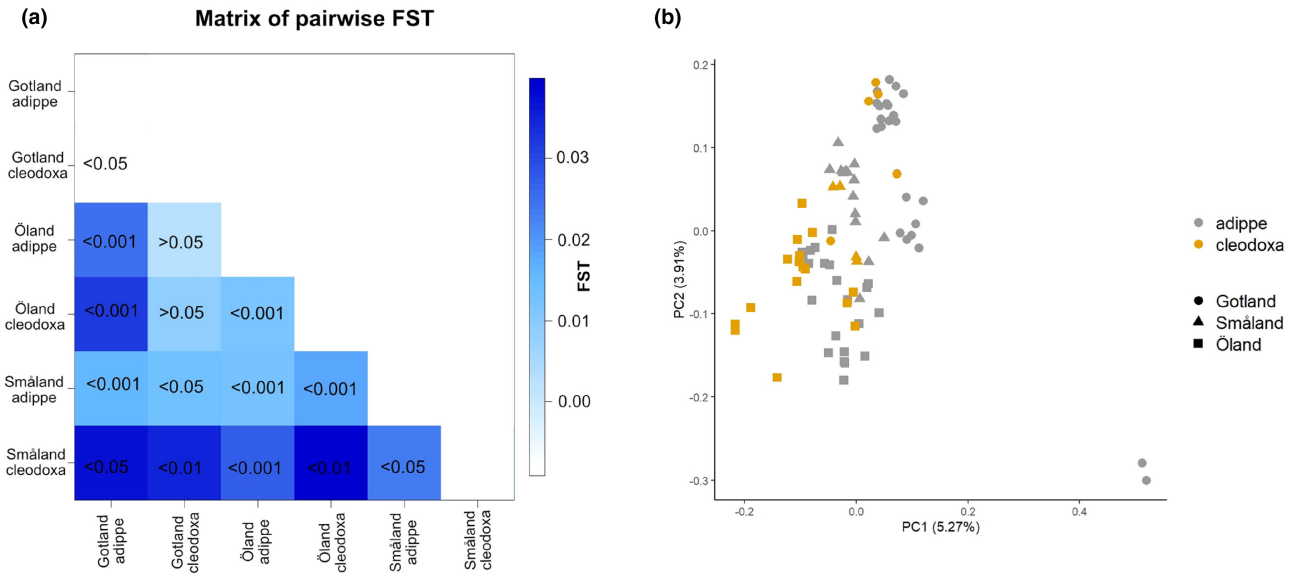

FIGURE 4 (a) Matrix of F_{ST} values for pairwise comparisons of individuals from colour morphs within and across populations. Darker colours indicate higher genetic differentiation between groups, *p*-values for each comparison are in the respective square. (b) Bi-plot according to PCA of ddRADseq data. Colours represent colour morphs, shapes represent populations.

more clearly. PERMANOVA results were in overall agreement with the outcome of the other analyses, suggesting a significant effect of population and colour morph on genetic structure (population, $F_{2,86}=1.91$, $p<.001$; colour morph, $F_{1,85}=1.39$, $p<.001$; interaction, $F_{2,85}=1.23$, $p<.001$). Overall, CAP analyses supported the genetic distinctiveness of the colour morphs for both the full dataset ($tr=0.70$, $p<.001$) and Öland ($tr=0.82$, $P<.001$, Figure S2). The cross-validation with leave-one-out method showed that the assignment success of the different morphs was 83.9% (73/87) for the full dataset, and 84.6% (33/39) for Öland (Table S5). We used only the Öland population separately for CAP analyses as it had a more balanced sampling for the respective colour morphs. For detailed results of PERMANOVA, PERMDISP and CAP, please see Results from PERMANOVA, PERMDISP and CAP in Appendix S1.

3.4 | Phylogenetic analysis

The phylogenetic (ML) tree revealed similarities in the genetic structure with results from F_{ST} and PERMANOVA analyses. Clades were primarily associated with sampling population, and an additional level of clustering was largely in line with colour morph identity within the populations, and this was least apparent on Gotland (Figure 5).

3.5 | Associations of phenotypic variables and the genetic structure

Performing db-RDA, the final selected models included colour morph, sex, source population (when analysing all three populations together), dorsal melanism, forewing length, the percentage of green in the ventral hindwing and the percentage of orange in all wings. The overall genetic structure was significantly associated with colour morph ($F_{1,72}=1.69$, $p<.001$), source population ($F_{1,72}=1.56$, $p<.001$) and sex ($F_{1,72}=1.53$, $p<.001$, Figure 6). The association with colour morph was consistent in all three populations. When analysing the three populations separately, we found that within Småland, the genetic structure was significantly associated only with colour morph ($F_{1,9}=1.26$, $p=.03$). On Öland, the genetic structure was significantly associated with colour morph ($F_{1,31}=1.71$, $p<.001$), sex ($F_{1,31}=1.72$, $p<.001$) and forewing length ($F_{1,31}=1.17$, $p=.03$). On Gotland, the genetic structure was significantly associated with colour morph ($F_{1,20}=1.13$, $p<.01$) and sex ($F_{1,20}=1.45$, $p<.001$) (Figure S3).

3.6 | Associations of colour morph with loci putatively under selection

Outlier analyses with Fdist and BayeScEnv suggested 116 ($p<.01$, Figure 7a) and 19 loci ($p<.05$, Figure 7b), respectively, associated with colour morph. Seventeen of these loci were identified using both methods. The overlapping loci were lying within the coding regions of one uncharacterized gene, one hypothetical gene, the *peptidyl-tRNA hydrolase 2* (*PTRH2*, a role in a functional protein synthesis in regulating cell survival and apoptosis (Sharkia et al., 2023)), the *peptidyl-prolyl cis-trans isomerase-like 2* (*PPIL2*, a role in spliceosome activity (Bai et al., 2021)), the *ribosome-releasing factor 2* (*RRF2*, involved in the ribosome's inherent catalytic activity in specific circumstances (Rodnina, 2013), and the *ultraviolet-sensitive visual pigment* gene; *UVRh1*, responsible for UV-vision in butterflies; Briscoe et al., 2010; Bybee et al., 2012) respectively. The remaining 11 loci could not be matched to any gene. We examined the protein-coding genes residing between the two SNPs flanking each outlier locus in Ensembl genome browser 110. There were 229 protein-coding genes in total at these candidate loci. The locus information for the outlier loci and the flanking SNPs, as well as the ID of the protein-coding genes can be found in Table 3. Please note that the *F. adippe* genome is not characterized, and protein-coding regions were annotated based on models. Moreover, the number of candidate genes is most probably higher than the actual number because none of the SNPs flanking the candidate outlier loci were themselves outliers, and the actual candidate loci should be much shorter in length. A denser genotyping could help identify the boundaries of the outlier loci.

We calculated the allele frequencies and assessed the genotype of individuals in each population at the outlier locus in *UVRh1* due to its potential role in colour perception. The allele distribution for *UVRh1* was different among the populations; the major allele frequency (MAF) was 0.52, 0.61 and 0.94 in Gotland, Öland and Småland, respectively (Table 4). Inbreeding coefficient (F_{IS}) values showed that all populations were significantly heterozygote deficient at the locus (Gotland: $F_{IS}=1$, $p<.001$; Öland: $F_{IS}=0.81$, $p<.001$; Småland $F_{IS}=1$, $p=.028$). We determined the genotype of the individuals for which the data was available. While the *adippe* morph had all three genotypes (T/T, A/A, T/A) at *UVRh1*, all *cleodoxa* individuals belonged to genotype T/T. In other words, MAF for individuals representing the *cleodoxa* morph was 1 regardless of their source population whereas the MAF for the *adippe* morph varied according to the sampling location ($0.40 \leq MAF \leq 0.93$, Table 5).

BayeScEnv analysis did not suggest any association of outlier loci with sex.

4 | DISCUSSION

The morphological and genomic analyses of three Swedish *F. adippe* populations revealed that the *adippe* morph was significantly larger, darker and had fewer green scales than the *cleodoxa* morph. The comparison of optical properties of the bright spots also provides evidence that UV reflectance of wing spots is about 15 times higher overall in *adippe* than *cleodoxa*, and about two times higher in female than in male *adippe*. Together, these findings suggest that the different morphs might represent alternative integrated phenotypes with

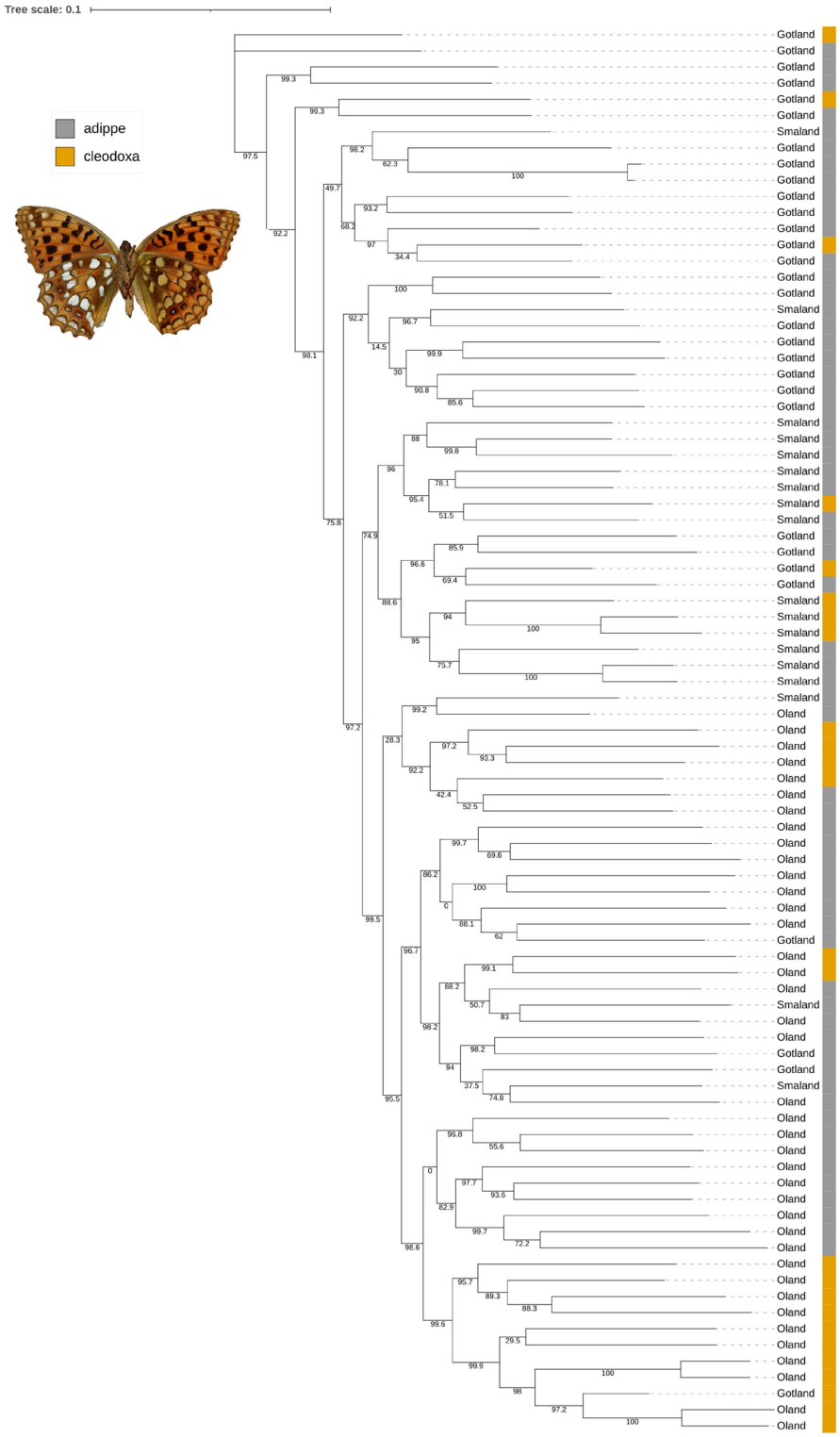

FIGURE 5 Maximum Likelihood inference tree according to ddRADseq data. Numbers on branches display bootstrap values. The top left corner shows a manipulated picture of *Fabriciana adippe* illustrating the ventral sides of both colour morphs, with the *adippe* morph on the left, and the *cleodoxa* morph on the right. Photo: Daniela Polic.

distinct trait value combinations, possibly constituting different fitness peaks in distinct microhabitats (discussed below). Importantly, the reported phenotypic associations with colour morph were largely consistent across all study populations, despite the clear population genetic structure indicated by our results. The results further show that colour morph identity was linked with the overall genetic structure, suggesting that the phenotypic differentiation between morphs reflects genetically based evolutionary modifications,

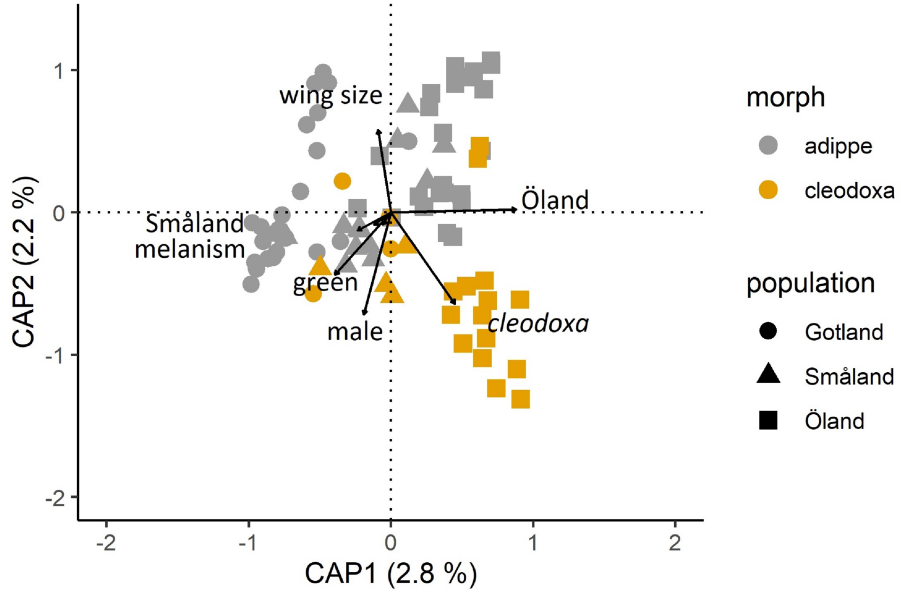

FIGURE 6 Bi-plots according to db-RDA of ddRADseq data showing associations of the genetic structure with colour morph identity, source population, sex and other phenotypic variables. Colours are according to colour morph, shapes represent source populations, and arrows show the direction of association of analysed variables with the genetic structure.

although we cannot rule out the possible role of plasticity integration. We also identified 17 outlier loci putatively under selection, including *UVRh1*, which were correlated with colour morph identity. Collectively, these results indicate that the phenotypic differentiation between colour morphs is likely adaptive and coincides with an underlying genomic differentiation that appears to have been driven by selection, although we cannot rule out the potential role of neutral processes, such as genetic drift.

4.1 | Colour morphs represent alternative integrated phenotypes

That the *adippe* and *cleodoxa* colour morphs appear to represent alternative phenotypes with distinct trait value combinations raises the question which functions and selective factors may have contributed to their evolutionary divergence. The evolution of phenotypic integration and trait associations can be driven by correlational selection, such as when susceptibility to visually oriented predators is reduced by specific combinations of for example prey colour pattern and avoidance behaviour (Brodie, 1992; Dingemanse et al., 2020; Forsman & Appelqvist, 1998), prey colour pattern and body size (Hagman & Forsman, 2003; Karpestam et al., 2014), or when the utilization of a certain habitat or niche favours specific associations of two or more phenotypic characteristics (Forsman et al., 2002; McKinnon & Pierotti, 2010). In *F. adippe*, the silvery *adippe* morph is likely better protected against predators in habitats with complex light conditions and visual backgrounds, such as forest glades, or clear-cut areas in woodland landscapes (Wilts et al., 2013). When at rest, the ventral wings are exposed, such that the iridescent silver scales can act as a mirror to the foliage, thus possibly enhancing camouflage and making the butterfly harder to detect for visually oriented predators (Kjernsmo et al., 2020). The specular reflection of light by the mother-of-pearl-like spots while flapping the wings might also complicate pursuit and capture of the butterfly in the interplay of light and shade. Conversely, such specular reflection might attract attention in open and visually more homogeneous grasslands, where the yellow *cleodoxa* morph with more green scales on the ventral hindwings might be better protected against detection and predation, as in the Green Hairstreak butterfly *Callophrys rubi* (Michielsen et al., 2010). However, since we did not specifically test for differences in predation avoidance between colour morphs in distinct microhabitats, our interpretations remain speculative. One way to evaluate the roles of predation would be to perform systematic detection and predation experiments, and to compare the escape behaviour and capture rates of the two morphs in contrasting environments.

That the silvery *adippe* form had both larger and darker wings might be another adaptation to shaded forest habitats, as this trait combination allows for more efficient absorption of sun light where the opportunities for sun-basking are limited (Bishop et al., 2016; Schweiger & Beierkuhnlein, 2016). A difference in wing size between colour morphs in *F. adippe* was also apparent in a study based on analyses of phenotypic data collected across a large spatial scale (>32° latitude and >47° longitude), with individuals belonging to the *adippe* morph having significantly larger wings than *cleodoxa* (see table S1 in Polic et al. (2023)). Still, firm evaluation of the hypothesis that these colour morphs represent alternative adaptive peaks associated with different microhabitats (i.e. forest vs. open habitats) would require to systematically study and compare habitat utilization where the two morphs occur in sympatry.

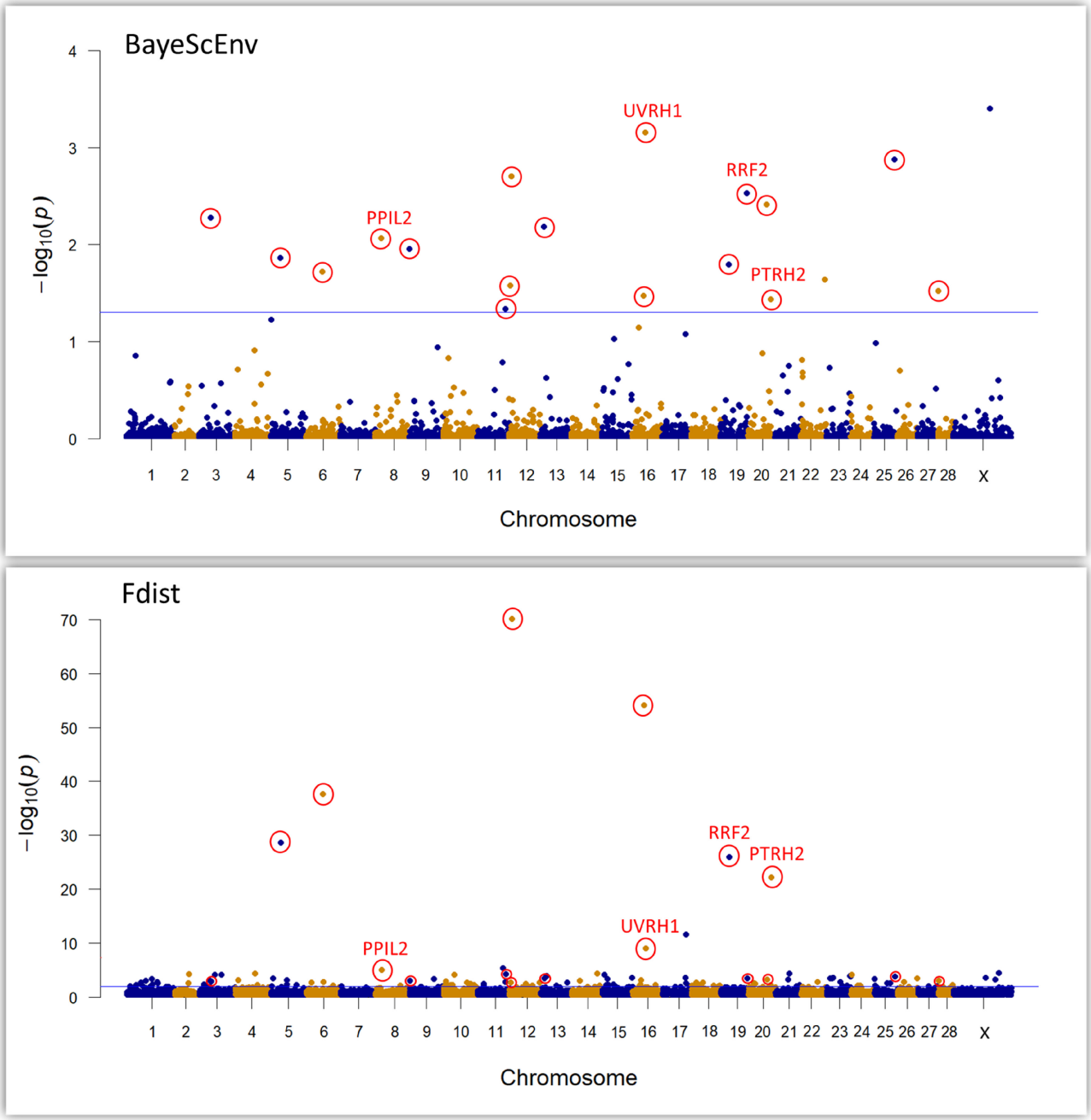

FIGURE 7 Outliers suggested by BayeScenv and Fdist. Blue lines represent the cut-off values ($p < .05$ for BayeScEnv and $p < .01$ for Fdist). Outliers identified by both methods are highlighted with encircled markers. Additionally, loci within a gene locus with known names are specifically indicated.

4.2 | Genetic differentiation between colour morphs

In principle, the type of alternative integrated phenotypes indicated by our results may represent the outcome of plasticity integration, which stems from developmental responses to environmental conditions experienced during development and growth (Pfennig et al., 2010; Whitman & Agrawal, 2009). However, that our results show signs of genetic differentiation associated with morphological dimensions instead points to a role of pleiotropic effects, supergenes, or linkage disequilibrium (McKinnon & Pierotti, 2010). Although a structuring according to colour morph was apparent, the structuring according to source population was more obvious. Please note that since the studied populations are geographically relatively isolated from each other, the genetic signature of colour morph might be masked by a stronger background genomic signal associated with source population. However, the genetic differentiation between colour morphs within each population remained

apparent (Figures 4–6, Figure S3). In parallel with the results from our analyses of phenotypic variation, db-RDA demonstrated that the genetic structure was associated not only with the two distinct morphs but also with forewing length (Öland only). In the mimetic butterfly *Hypolimnas misippus*, from the same family as *F. adippe* (Nymphalidae), distinct colour pattern variation is correlated with differences in body size, presumably owing to a supergene linked to several loci (Gordon & Smith, 1998). A recent study on the polymorphic *H. numata* found a supergene responsible for several independent loci associated with distinct wing pattern characteristics (Jay et al., 2022). An association in the grasshopper species *Tetrix undulata* of maternal colour morph with offspring body size variations, regardless of differences in environmental conditions during rearing, also suggests a genetic link between these traits (Ahnesjö & Forsman, 2003).

Although we were unable to test for genetic correlations, as the genome for *F. adippe* has not been characterized, it is possible that the genomic regions associated with colour morph identity and wing size are linked. Both pleiotropy and linkage disequilibrium could be responsible for patterns where traits do not vary independently of one another (Falconer & Mackay, 1996; Wright, 1984). A stable maintenance of genetic correlations might indicate pleiotropic effects, while physically linked loci might be expected to break up or reduce the associations between characteristics within a few generations due to recombination and segregation, although linkage equilibrium is expected to be reached slowly for linked genes (Conner, 2002). However, strong selection or tight linkage due to physical proximity can prevent allele separation via recombination (Li & Nei, 1974). Linkage disequilibrium can also be maintained in deep evolutionary time through supergene formation (Fisher, 1939; Ford, 1965; Küpper et al., 2016; Nabours, 1929; Thompson & Jiggins, 2014). That the associations of colour morph with melanism, wing size, the amount of green scales and the presence of iridescent structures that reflect UV-light were evident across all studied populations, despite that populations were genetically distinct from each other, might indicate that trait correlations are rather stable and likely have existed since before populations spread from the Swedish mainland to the islands. That the majority of outlier loci, including *UVRh1*, reside in separate chromosomes might suggest some pleiotropic involvement in these integrated phenotypes. Please note that some outliers lie on the same chromosomes, which suggests that there is some physical linkage between these SNPs, at least at the chromosomal level. However, since we are unable to identify the main loci responsible for the colour polymorphism (silvery *adippe* vs. yellow *cleodoxa*) and many more genes might contribute to the aforementioned phenotypes, these genes could be in linkage disequilibrium with the detected outlier loci. Although we can only speculate about the exact genetic architecture, we suggest that linkage disequilibrium likely underlies the observed trait value combinations, as our results point to that many genes are involved in the distinction of colour morphs (e.g. overall genetic differentiation between morphs).

4.3 | Prevalence and mediators of genetic differentiation between colour morphs

Our study provides rare empirical evidence for an overall genetic divergence that is correlated with phenotypic (wing size, colour pattern, and UV reflectance) variation in the High Brown Fritillary. While several other studies discovered genetic divergences that coincided with colour pattern variation in other species, our study stands out as it shows a general genetic difference between colour morphs occurring in the same population. For example, the wood tiger moth *Parasemia plantaginis* exhibits geographical differences in hindwing warning coloration, with high levels of differentiation between populations at contrasting margins of the species' distribution range, and a weaker genetic divergence coinciding with hindwing coloration (Hegna et al., 2015). However, the tiger moth study covered a much larger spatial scale, and colour variation was highly correlated with geographic location. Similarly, a study on the polymorphic ballan wrasse *Labrus bergylta* revealed an overall genetic structuring along a latitudinal gradient that coincides with morph frequencies (Casas et al., 2021). In the highly polymorphic strawberry poison-dart frog *Dendrobates pumilio*, the genetic distance between populations is associated with phenotypic differences rather than with geographic distance, however, divergent phenotypes are allopatric in this species (Wang & Summers, 2010). Similar to the findings in our present study of butterflies, studies of genetic structure of marine taxa with sympatric distinct phenotypes, for example, in the arc-eye hawkfish *Paracirrhites arcatus*, the sea urchin *Paracentrotus gaimardi* or the sea anemone *Parazoanthus axinellae*, report on genomic associations with colour morphs, however, they used fewer nuclear and mitochondrial genomic regions (Calderon et al., 2010; Villamor et al., 2020; Whitney et al., 2018).

The existence of distinct and (partially) genetically diverged colour morphs in a species has previously been interpreted as a sign of reproductive isolation (e.g. Boratynski et al., 2014; Casas et al., 2021), which can be mediated through assortative mating, or as a result of spatial sorting (Van Belleghem et al., 2016). If morphs utilize different habitats, assortative mating may occur as a by-product even in the absence of specific mate preferences or avoidance behaviours (Berggren et al., 2012; Calderon et al., 2010; Shine et al., 2011). The silvery patterns in the *adippe* morph might be important for intraspecific signalling, where the flashing of the reflective spots in sunlight might facilitate conspecific perception and attract the attention of potential mating partners, a phenomenon observed in various taxa (Mouchet & Vukusic, 2018; Vukusic & Sambles, 2003). Our finding of sex-based differences in UV reflectance suggests a role in intraspecific communication, such as mate choice or intra-sexual signalling. Female *adippe* butterflies had roughly double the UV reflectance of males, potentially indicating male mate choice, such as observed in *Bicyclus anynana*, where females have more hindwing eyespots than males, and males, but not females, learn to choose mates based on the number of these spots (Westerman et al., 2014). Although many

butterfly species exhibit female (Kemp, 2008; Papke et al., 2007; Silberglied, 1984) or mutual (Westerman et al., 2014) mate choice, there are many documented cases of male mate choice. Such examples include *Pieris napi* and *P. rapae* where UV reflectance is higher in females, and males actively search for females, with UV reflection playing an important role in mate localization, recognition and choice (Fukano et al., 2012; Stella et al., 2018). Another case is *Colias philodice eriphyle*, where males choose females based on wing melanisation (Ellers & Boggs, 2003). We propose that *F. adippe* males might find and choose females based on the bright spots on the ventral hindwings, however, further studies on mating behaviour are needed to evaluate this proposition.

As *F. adippe* is a non-model organism, our data cannot identify with certainty the specific mechanisms shaping the phenotypic and genetic differentiation between distinct colour morphs documented in this species. However, we propose that both genetic and environmental variables influence the genomic architecture of the colour polymorphism. Because each distinct morph might be better suited for different microhabitats within the same population (see Section 4.1), diverging mating signals and preferences might have evolved, thereby potentially enabling the occupancy of a broader niche (Nosil & Feder, 2012). This is supported by the detection of an outlier locus appearing to be under divergent selection associated with colour morph identity, that is, *ultraviolet-sensitive visual pigment* (*UVRh1*). This gene plays an important role in intraspecific signalling, especially for mate choice correlated with wing colouration that reflects UV light, as reported for polymorphic *Heliconius* butterflies, a tropical genus in the family Nymphalidae, the same as *F. adippe* (Bybee et al., 2012; Chamberlain et al., 2009). In *Heliconius* butterflies, another *UVRh* opsin, which has formed as a duplication of *UVRh1*, is associated with perceiving the colour yellow in wings and there is evidence that UV receptors in their eyes have co-evolved with wing pigmentation (Briscoe et al., 2010).

Our demonstrations that the iridescent spots of the *adippe* morph (but barely the corresponding yellow spots on the *cleodoxa* morph) reflect UV light, that morphs differ in *UVRh1* genotypes, and that there is an overall genetic divergence between colour morphs, suggest that selective mating is involved in the evolution and maintenance of the colour polymorphism in the High Brown Fritillary. That all sampled populations showed a significant heterozygote deficiency at the outlier locus coding for *UVRh1* (Table 4) also points towards non-random mating, as inbreeding decreases the frequency of heterozygotes (Gaffney et al., 1990; Rousset & Raymond, 1995). It should be mentioned that all possible genotypes at *UVRh1* were present in *adippe*, while only one (T/T) was found in *cleodoxa* (Tables 4 and 5), possibly indicating that the in Sweden rarer *cleodoxa* morph might be more selective. This is similar to what has been documented for *Heliconius cydno* butterflies, which show different gene expression levels between yellow and white butterflies at a locus that also plays a dominant role in mediating assortative mating (Chamberlain et al., 2009; Westerman, VanKuren, et al., 2018). In *H. cydno*, the distinct colour patterns have a mimetic function across geographic races and assortative mating seems to contribute to ongoing ecological speciation in this system (Chamberlain et al., 2009). Due to the very similar sympatric wing pattern polymorphism and assortative mating system, we carefully point towards the possibility of ecological speciation in *F. adippe*. Still, it remains an open question whether the here documented phenotypic and genomic differentiation between these colour morphs represents an early stage of ongoing evolutionary diversification. That *F. adippe*'s sister species, *F. niobe*, shares a similar colour polymorphism with the nominate form *F. niobe f. niobe* exhibiting iridescent spots on the ventral hindwings, and *F. niobe f. eris* displaying yellow spots, seems to suggest that this colour polymorphism might be ancient (Eliasson et al., 2005; Tolman & Lewington, 2012). Such homologous polymorphisms highlight that multiple species may react similarly to analogous selective pressures (convergent evolution), and emphasize the benefits and the phylogenetic antiquity of phenotypic intraspecific trait variation as a response to shared prevailing selective regimes (Forsman, 2016; Mayr, 1963).

5 | CONCLUSIONS AND FUTURE DIRECTIONS

We provide phenotypic and molecular evidence that the *F. adippe* colour morphs *adippe* and *cleodoxa* represent two genetically distinct and alternative integrated phenotypes. The overall genetic differentiation between morphs is in contrast to many other examples of colour polymorphism, where alternative colour pattern variants have been linked to differences in one or a few genes as in the Soay sheep (Gratten et al., 2007) and the black-headed bulbul (Shakya et al., 2021), or with a structural genomic change in the form of a super gene (chromosome inversion), as in, for example, *Heliconius* butterflies (Joron et al., 2011), the common ruff (Lamichhaney et al., 2016), and redpoll finches (Funk et al., 2021). Our discovery of the genetic diversification of the UV-sensitive visual pigment together with the demonstration of higher reflectance in the UV range of the iridescent spots on the wings of the *adippe* morph, particularly in females, points to a possible role of intraspecific communication and sexual selection as a contributing driver of the evolution of genetic and phenotypic integration within and differentiation between colour morphs, similar to what we see in *H. cydno* butterflies (Chamberlain et al., 2009, Westerman, VanKuren, et al., 2018). In addition, we propose that divergent selection for thermoregulation and predator avoidance associated with differences in microhabitat use may also have contributed to the separation in size, darkness and iridescence between morphs.

Our study spurs several questions about the evolutionary dynamics of this polymorphism. For example, additional sampling from other parts of the distributional range may help identify environmental drivers of diversification and inform whether the differences between morphs are general or context specific. Studies of habitat use, thermoregulation and mate choice, together with comparisons of viability of offspring from pure and mixed parental combinations

in staged mating experiments, and comparisons of detectability and predation risk of the morphs in different habitats can help identify the underlying selection pressures. Finally, whole-genome sequencing may identify genomic regions and possible chromosomal re-arrangements responsible for differences in colour patterns and other traits.

AUTHOR CONTRIBUTIONS

DP, AF, YY and MF designed the study. Funding was secured by AF, MF, DP and YY. DP, MF and YY collected the samples. DP and YY performed the laboratory work. SM conducted the reflectance measurements. DP, YY and AF analysed the data. DP and AF wrote the first draft of the manuscript. All authors contributed to the final version and approved the submitted manuscript.

ACKNOWLEDGEMENTS

We thank Paulo Ricardo Ribeiro Cardoso for his help with taking pictures of the butterflies and measuring wing size and colours, and Roger Vila for providing the facilities for photographing the butterflies. We thank Marko Mutanen for providing the laboratory facilities for preparing the ddRADseq libraries, and Kyung Min Lee and Laura Törmälä for help in the laboratory. Thanks to Kyung Min Lee for help with preparing the catalogue of loci. Two anonymous reviewers provided valuable comments on the manuscript. The authors acknowledge support from the National Genomics Infrastructure in Stockholm funded by Science for Life Laboratory, the Knut and Alice Wallenberg Foundation and the Swedish Research Council, and NAISS for assistance with massively parallel sequencing and access to the UPPMAX computational infrastructure. The computations were performed under project b2017043. Funding was provided by Linnaeus University (to AF and MF), The Swedish Research Council FORMAS (to AF and MF, 2018-02846), The Carl Trygger Foundation (to MF), Erasmus+ mobility program (to DP and YY) and Entomologiska Föreningen Stockholm (to DP).

CONFLICT OF INTEREST STATEMENT

The authors have no conflicts of interest to disclose.

DATA AVAILABILITY STATEMENT

Raw ddRAD sequences can be found in the NCBI SRA under the BioProject ID PRJNA838593 (accession codes: SRR19224314–SRR19224384 (Polic, Yıldırım, Merilaita, et al., 2022)). The previously published raw data were retrieved from the project PRJNA70744 (accession codes: SRP309715, SRP309715, SRP309715, SRP309715, SRP309715, SRP309715, SRP309715, SRP309715, SRP309715, SRP309715, SRP309715, SRP309715, SRP309715 and SRP309715 (Polic, Yıldırım, Lee, et al., 2022)).

ORCID

Daniela Polic https://orcid.org/0000-0001-6168-6489
Yeşerin Yıldırım https://orcid.org/0000-0002-0431-8417
Anders Forsman https://orcid.org/0000-0001-9598-7618

REFERENCES

Ahnesjö, J., & Forsman, A. (2003). Correlated evolution of colour pattern and body size in polymorphic pygmy grasshoppers, *Tetrix undulata*. *Journal of Evolutionary Biology*, *16*, 1308–1318.

Anderson, M. J. (2006). Distance-based tests for homogeneity of multivariate dispersions. *Biometrics*, *62*, 245–253.

Anderson, M. J., & Willis, T. J. (2003). Canonical analysis of principal coordinates: A useful method of constrained ordination for ecology. *Ecology*, *84*, 511–525.

Andersson, L. (2001). Genetic dissection of phenotypic diversity in farm animals. *Nature Reviews Genetics*, *2*, 130–138.

Andrews, K. R., Good, J. M., Miller, M. R., Luikart, G., & Hohenlohe, P. A. (2016). Harnessing the power of RADseq for ecological and evolutionary genomics. *Nature Reviews Genetics*, *17*, 81–92.

Bai, R., Wan, R., Wang, L., Xu, K., Zhang, Q., Lei, J., & Shi, Y. (2021). Structure of the activated human minor spliceosome. *Science*, *371*, eabg0879.

Berggren, H., Tinnert, J., & Forsman, A. (2012). Spatial sorting may explain evolutionary dynamics of wing polymorphism in pygmy grasshoppers. *Journal of Evolutionary Biology*, *25*, 2126–2138.

Berwaerts, K., Van Dyck, H., & Aerts, P. (2002). Does flight morphology relate to flight performance? An experimental test with the butterfly *Pararge aegeria*. *Functional Ecology*, *16*, 484–491.

Bishop, T. R., Robertson, M. P., Gibb, H., van Rensburg, B. J., Braschler, B., Chown, S. L., Foord, S. H., Munyai, T. C., Okey, I., Tshivhandekano, P. G., Werenkraut, V., & Parr, C. L. (2016). Ant assemblages have darker and larger members in cold environments. *Global Ecology and Biogeography*, *25*, 1489–1499.

Bond, A. B. (2007). The evolution of color polymorphism: Crypticity, searching images, and apostatic selection. *Annual Review of Ecology, Evolution, and Systematics*, *38*, 489–514.

Boratynski, Z., Brito, J. C., Campos, J. C., Karala, M., & Mappes, T. (2014). Large spatial scale of the phenotype-environment color matching in two cryptic species of African desert jerboas (Dipodidae: Jaculus). *PLoS One*, *9*, e94342.

Brien, M. N., Orteu, A., Yen, E. C., Galarza, J. A., Kirvesoja, J., Pakkanen, H., Wakamatsu, K., Jiggins, C. D., & Mappes, J. (2023). Colour polymorphism associated with a gene duplication in male wood tiger moths. *bioRxiv*. https://doi.org/10.1101/2022.04.29.490025

Briscoe, A. D., Bybee, S. M., Bernard, G. D., Yuan, F., Sison-Mangus, M. P., Reed, R. D., Warren, A. D., Llorente-Bousquets, J., & Chiao, C.-C. (2010). Positive selection of a duplicated UV-sensitive visual pigment coincides with wing pigment evolution in Heliconius butterflies. *Proceedings of the National Academy of Sciences of the United States of America*, *107*, 3628–3633.

Brodie, E. D. (1992). Correlational selection for color pattern and antipredator behavior in the garter snake *Thamnophis ordinoides*. *Evolution*, *46*, 1284–1298.

Brusa, O., Bellati, A., Meuche, I., Mundy, N. I., Pröhl, H., & Rocha, L. (2013). Divergent evolution in the polymorphic granular poison-dart frog, *Oophaga granulifera*: Genetics, coloration, advertisement calls and morphology. *Journal of Biogeography*, *40*, 394–408.

Bybee, S. M., Yuan, F., Ramstetter, M. D., Llorente-Bousquets, J., Reed, R. D., Osorio, D., & Briscoe, A. D. (2012). UV photoreceptors and UV-yellow wing pigments in Heliconius butterflies allow a color signal to serve both mimicry and intraspecific communication. *The American Naturalist*, *179*, 38–51.

Caillaud, M. C., & Losey, J. E. (2010). Genetics of color polymorphism in the pea aphid, *Acyrthosiphon pisum*. *Journal of Insect Science*, *10*, 1–13.

Calderon, I., Ventura, C. R., Turon, X., & Lessios, H. A. (2010). Genetic divergence and assortative mating between colour morphs of the sea urchin *Paracentrotus gaimardi*. *Molecular Ecology*, *19*, 484–493.

Casas, L., Saenz-Agudelo, P., Villegas-Rios, D., Irigoien, X., & Saborido-Rey, F. (2021). Genomic landscape of geographically structured

colour polymorphism in a temperate marine fish. *Molecular Ecology*, *30*, 1281–1296.
Catchen, J., Hohenlohe, P. A., Bassham, S., Amores, A., & Cresko, W. A. (2013). Stacks: An analysis tool set for population genomics. *Molecular Ecology*, *22*, 3124–3140.
Catchen, J. M., Amores, A., Hohenlohe, P., Cresko, W., & Postlethwait, J. H. (2011). Stacks: Building and genotyping LociDe NovoFrom short-read sequences. *G3 (Bethesda)*, *1*, 171–182.
Challi, R. J., Kumar, S., Dasmahapatra, K. K., Jiggins, C. D., & Blaxter, M. (2016). Lepbase: The lepidopteran genome database. *bioRxiv*. https://doi.org/10.1101/056994
Chamberlain, N. L., Hill, R. I., Kapan, D. D., Gilbert, L. E., & Kronforst, M. R. (2009). Polymorphic butterfly reveals the missing link in ecological speciation. *Science*, *326*, 847–850.
Clench, H. K. (1966). Behavioral thermoregulation in butterflies. *Ecology*, *47*, 1021–1034.
Conner, J. K. (2002). Genetic mechanisms of floral trait correlations in a natural population. *Nature*, *420*, 407–410.
de Villemereuil, P., & Gaggiotti, O. E. (2015). A new FST-based method to uncover local adaptation using environmental variables. *Methods in Ecology and Evolution*, *6*, 1248–1258.
Dingemanse, N. J., Barber, I., & Dochtermann, N. A. (2020). Non-consumptive effects of predation: Does perceived risk strengthen the genetic integration of behaviour and morphology in stickleback? *Ecology Letters*, *23*, 107–118.
Eliasson, C., Ryrholm, N., & Gärdenfors, U. (2005). *Nationalnyckeln till Sveriges flora och fauna. Fjärilar. Dagfjärilar, Hesperiidae – Nymphalidae*. Artdatabanken SLU.
Ellers, J., & Boggs, C. L. (2003). The evolution of wing color: Male mate choice opposes adaptive wing color divergence in *Colias* butterflies. *Evolution*, *57*, 1100–1106.
Excoffier, L., Laval, G., & Schneider, S. (2005). Arlequin (version 3.0): An integrated software package for population genetics data analysis. *Evolutionary Bioinformatics*, *1*, 47–50.
Excoffier, L., & Lischer, H. E. (2010). Arlequin suite ver 3.5: A new series of programs to perform population genetics analyses under Linux and windows. *Molecular Ecology Resources*, *10*, 564–567.
Falconer, D., & Mackay, T. (1996). *Introduction to quantitative genetics* (4th ed.). Longman.
Finkbeiner, S. D., & Briscoe, A. D. (2021). True UV color vision in a female butterfly with two UV opsins. *Journal of Experimental Biology*, *224*, jeb242802.
Fisher, R. A. (1930). The evolution of dominance in certain polymorphic species. *American Naturalist*, *64*, 385–406.
Fisher, R. A. (1939). Selective forces in wild populations of *Paratettix texanus*. *Annals of Eugenics*, *9*, 109–122.
Ford, E. B. (1945). Polymorphism. *Biological Reviews*, *20*, 73–88.
Ford, E. B. (1965). *Genetic polymorphism*. Faber & Faber.
Forsman, A. (2016). Is colour polymorphism advantageous to populations and species? *Molecular Ecology*, *25*, 2693–2698.
Forsman, A., Ahnesjö, J., Caesar, S., & Karlsson, M. (2008). A model of ecological and evolutionary consequences of color polymorphism. *Ecology*, *89*, 34–40.
Forsman, A., & Appelqvist, S. (1998). Visual predators impose correlational selection on prey color pattern and behavior. *Behavioral Ecology*, *9*, 409–413.
Forsman, A., Polic, D., Sunde, J., Betzholtz, P. E., & Franzén, M. (2020). Variable colour patterns indicate multidimensional, intraspecific trait variation and ecological generalization in moths. *Ecography*, *43*, 823–833.
Forsman, A., Ringblom, K., Civantos, E., & Ahnesjö, J. (2002). Coevolution of color pattern and thermoregulatory behavior in polymorphic pygmy grasshoppers *Tetrix undulata*. *Evolution*, *56*, 349–360.
Forsman, A., & Wennersten, L. (2016). Inter-individual variation promotes ecological success of populations and species: Evidence from experimental and comparative studies. *Ecography*, *39*, 630–648.
Fruciano, C., Franchini, P., Kovacova, V., Elmer, K. R., Henning, F., & Meyer, A. (2016). Genetic linkage of distinct adaptive traits in sympatrically speciating crater lake cichlid fish. *Nature Communications*, *7*, 1–8.
Fukano, Y., Satoh, T., Hirota, T., Nishide, Y., & Obara, Y. (2012). Geographic expansion of the cabbage butterfly (*Pieris rapae*) and the evolution of highly UV-reflecting females. *Insect Science*, *19*, 239–246.
Funk, E. R., Mason, N. A., Pálsson, S., Albrecht, T., Johnson, J. A., & Taylor, S. A. (2021). A supergene underlies linked variation in color and morphology in a Holarctic songbird. *Nature Communications*, *12*, 6833.
Gaffney, P. M., Scott, T. M., Koehn, R. K., & Diehl, W. J. (1990). Interrelationships of heterozygosity, growth rate and heterozygote deficiencies in the coot clam, *Mulinia lateralis*. *Genetics*, *124*, 687–699.
Garner, B. A., Hoban, S., & Luikart, G. (2020). IUCN Red list and the value of integrating genetics. *Conservation Genetics*, *21*, 795–801.
Ghisbain, G., Lozier, J. D., Rahman, S. R., Ezray, B. D., Tian, L., Ulmer, J. M., Heraghty, S. D., Strange, J. P., Rasmont, P., & Hines, H. M. (2020). Substantial genetic divergence and lack of recent gene flow support cryptic speciation in a colour polymorphic bumble bee (*Bombus bifarius*) species complex. *Systematic Entomology*, *45*, 635–652.
Gordon, I. J., & Smith, D. A. S. (1998). Body size and colour-pattern genetics in the polymorphic mimetic butterfly *Hypolimnas misippus* (L.). *Heredity*, *80*, 62–69.
Gorley, A., & Clarke, K. (2008). *PERMANOVA+ for PRIMER: Guide to software and statistical methods*. PRIMER-E.
Gorley, C. K., & Clarke, K. (2006). *PRIMER v6: user manual/tutorial*. PRIMER-E.
Gratten, J., Beraldi, D., Lowder, B. V., McRae, A. F., Visscher, P. M., Pemberton, J. M., & Slate, J. (2007). Compelling evidence that a single nucleotide substitution in *TYRP1* is responsible for coat-colour polymorphism in a free-living population of Soay sheep. *Proceedings of the Royal Society B: Biological Sciences*, *274*, 619–626.
Gray, S. M., & McKinnon, J. S. (2007). Linking color polymorphism maintenance and speciation. *Trends in Ecology & Evolution*, *22*, 71–79.
Hagman, M., & Forsman, A. (2003). Correlated evolution of conspicuous coloration and body size in poison frogs (Dendrobatidae). *Evolution*, *57*, 2904–2910.
Hegna, R. H., Galarza, J. A., & Mappes, J. (2015). Global phylogeography and geographical variation in warning coloration of the wood tiger moth (*Parasemia plantaginis*). *Journal of Biogeography*, *42*, 1469–1481.
Hoekstra, H. E., Drumm, K. E., & Nachman, M. W. (2004). Ecological genetics of adaptive color polymorphism in pocket mice: Geographic variation in selected and neutral genes. *Evolution*, *58*, 1329–1341.
Hoekstra, H. E., & Nachman, M. W. (2003). Different genes underlie adaptive melanism in different populations of rock pocket mice. *Molecular Ecology*, *12*, 1185–1194.
Huey, R. B., & Kingsolver, J. G. (1989). Evolution of thermal sensitivity of ectotherm performance. *Trends in Ecology & Evolution*, *4*, 131–135.
Hughes, A. R., Inouye, B. D., Johnson, M. T., Underwood, N., & Vellend, M. (2008). Ecological consequences of genetic diversity. *Ecology Letters*, *11*, 609–623.
James, G., Witten, D., Hastie, T., & Tibshirani, R. (2013). *An introduction to statistical learning*. Springer.
Jay, P., Leroy, M., Le Poul, Y., Whibley, A., Arias, M., Chouteau, M., & Joron, M. (2022). Association mapping of colour variation in a butterfly provides evidence that a supergene locks together a cluster of adaptive loci. *Philosophical Transactions of the Royal Society, B: Biological Sciences*, *377*, 20210193.
Jeong, H., Baran, N. M., Sun, D., Chatterjee, P., Layman, T. S., Balakrishnan, C. N., Maney, D. L., & Yi, S. V. (2022). Dynamic molecular evolution

of a supergene with suppressed recombination in white-throated sparrows. *eLife*, *11*, e79387.

Jiang, Y., Bolnick, D. I., & Kirkpatrick, M. (2013). Assortative mating in animals. *The American Naturalist*, *181*, E125–E138.

Joron, M., Frezal, L., Jones, R. T., Chamberlain, N. L., Lee, S. F., Haag, C. R., Whibley, A., Becuwe, M., Baxter, S. W., Ferguson, L., Wilkinson, P. A., Salazar, C., Davidson, C., Clark, R., Quail, M. A., Beasley, H., Glithero, R., Lloyd, C., Sims, S., … ffrench-Constant, R. H. (2011). Chromosomal rearrangements maintain a polymorphic supergene controlling butterfly mimicry. *Nature*, *477*, 203–206.

Kalarus, K., Skórka, P., Halecki, W., Jirak, A., Kajzer-Bonk, J., & Nowicki, P. (2013). Within-patch mobility and flight morphology reflect resource use and dispersal potential in the dryad butterfly Minois dryas. *Journal of Insect Conservation*, *17*, 1221–1228.

Karpestam, E., Merilaita, S., & Forsman, A. (2014). Body size influences differently the detectabilities of colour morphs of cryptic prey. *Biological Journal of the Linnean Society*, *113*, 112–122.

Kemp, D. J. (2008). Female mating biases for bright ultraviolet iridescence in the butterfly *Eurema hecabe* (Pieridae). *Behavioral Ecology*, *19*, 1–8.

Kingsolver, J. G. (1985). Thermoregulatory significance of wing melanization in Pieris butterflies (Lepidoptera: Pieridae): Physics, posture, and pattern. *Oecologia*, *66*, 546–553.

Kingsolver, J. G., & Koehl, M. A. R. (1985). Aerodynamics, thermoregulation, and the evolution of INSECT wings: Differential scaling and evolutionary change. *Evolution*, *39*, 488–504.

Kjernsmo, K., Whitney, H. M., Scott-Samuel, N. E., Hall, J. R., Knowles, H., Talas, L., & Cuthill, I. C. (2020). Iridescence as camouflage. *Current Biology*, *30*, 551–555.

Kronforst, M. R., Young, L. G., Kapan, D. D., McNeely, C., O'Neill, R. J., & Gilbert, L. E. (2006). Linkage of butterfly mate preference and wing color preference cue at the genomic location of wingless. *Proceedings of the National Academy of Sciences of the United States of America*, *103*, 6575–6580.

Kunte, K., Zhang, W., Tenger-Trolander, A., Palmer, D. H., Martin, A., Reed, R. D., Mullen, S. P., & Kronforst, M. R. (2014). Doublesex is a mimicry supergene. *Nature*, *507*, 229–232.

Küpper, C., Stocks, M., Risse, J. E., Dos Remedios, N., Farrell, L. L., McRae, S. B., Morgan, T. C., Karlionova, N., Pinchuk, P., & Verkuil, Y. I. (2016). A supergene determines highly divergent male reproductive morphs in the ruff. *Nature Genetics*, *48*, 79–83.

Lamichhaney, S., Fan, G., Widemo, F., Gunnarsson, U., Thalmann, D. S., Hoeppner, M. P., Kerje, S., Gustafson, U., Shi, C., Zhang, H., Chen, W., Liang, X., Huang, L., Wang, J., Liang, E., Wu, Q., Lee, S. M.-Y., Xu, X., Höglund, J., … Andersson, L. (2016). Structural genomic changes underlie alternative reproductive strategies in the ruff (*Philomachus pugnax*). *Nature Genetics*, *48*, 84–88.

Lancaster, L. T., McAdam, A. G., Hipsley, C. A., & Sinervo, B. R. (2014). Frequency-dependent and correlational selection pressures have conflicting consequences for assortative mating in a color-polymorphic lizard, uta stansburiana. *The American Naturalist*, *184*, 188–197.

Lande, R. (1998). Anthropogenic, ecological and genetic factors in extinction and conservation. *Population Ecology*, *40*, 259–269.

Lande, R., & Arnold, S. J. (1983). The measurement of selection on correlated characters. *Evolution*, *37*, 1210–1226.

Lank, D. B. (2002). Diverse processes maintain plumage polymorphisms in birds. *Journal of Avian Biology*, *33*, 327–330.

Lee, K. M., Kivelä, S. M., Ivanov, V., Hausmann, A., Kaila, L., Wahlberg, N., & Mutanen, M. (2018). Information dropout patterns in restriction site associated DNA phylogenomics and a comparison with multilocus sanger data in a species-rich moth genus. *Systematic Biology*, *67*, 925–939.

Legendre, P., & Anderson, M. J. (1999). Distance-based redundancy analysis: testing multispecies responses in multifactorial ecological experiments. *Ecological Monographs*, *69*, 1–24.

Lessells, C., & Boag, P. T. (1987). Unrepeatable repeatabilities: A common mistake. *The Auk*, *104*, 116–121.

Letunic, I., & Bork, P. (2019). Interactive tree of life (iTOL) v4: Recent updates and new developments. *Nucleic Acids Research*, *47*, W256–W259.

Li, W.-H., & Nei, M. (1974). Stable linkage disequilibrium without epistasis in subdivided populations. *Theoretical Population Biology*, *6*, 173–183.

Lohse, K., Vila, R., Hayward, A., Laetsch, D. R., Wahlberg, N., & Darwin Tree of Life Consortium. (2022). The genome sequence of the high brown fritillary, *Fabriciana adippe* (Dennis & Schiffermüller, 1775). *Wellcome Open Research*, *7*, 298.

Mayr, E. (1963). *Animal species and evolution*. Harvard University Press.

McArdle, B. H., & Anderson, M. J. (2001). Fitting multivariate models to community data: A comment on distance-based redundancy analysis. *Ecology*, *82*, 290–297.

McKinnon, J. S., & Pierotti, M. E. (2010). Colour polymorphism and correlated characters: Genetic mechanisms and evolution. *Molecular Ecology*, *19*, 5101–5125.

McLean, C. A., & Stuart-Fox, D. (2014). Geographic variation in animal colour polymorphisms and its role in speciation. *Biological Reviews*, *89*, 860–873.

McLean, C. A., Stuart-Fox, D., & Moussalli, A. (2015). Environment, but not genetic divergence, influences geographic variation in colour morph frequencies in a lizard. *BMC Evolutionary Biology*, *15*, 156.

Michielsen, K., De Raedt, H., & Stavenga, D. G. (2010). Reflectivity of the gyroid biophotonic crystals in the ventral wing scales of the green hairstreak butterfly, *Callophrys rubi*. *Journal of The Royal Society Interface*, *7*, 765–771.

Mouchet, S. R., & Vukusic, P. (2018). Structural colours in lepidopteran scales. *Advances in Insect Physiology*, *54*, 1–53.

Nabours, R. K. (1929). The genetics of the Tettigidae. *Bibliographia Genetica*, *5*, 27–104.

Nakagawa, S., & Schielzeth, H. (2010). Repeatability for Gaussian and non-Gaussian data: A practical guide for biologists. *Biological Reviews*, *85*, 935–956.

Nguyen, L.-T., Schmidt, H. A., von Haeseler, A., & Minh, B. Q. (2015). IQ-TREE: A fast and effective stochastic algorithm for estimating maximum-likelihood phylogenies. *Molecular Biology and Evolution*, *32*, 268–274.

Nijhout, H. F. (1991). *The development and evolution of butterfly wing patterns*. Smithsonian Institute Press.

Nosil, P., & Feder, J. L. (2012). Genomic divergence during speciation: Causes and consequences. *Philosophical Transactions of the Royal Society B*, *367*, 332–342.

Ogawa, Y., Kinoshita, M., Stavenga, D. G., & Arikawa, K. (2013). Sex-specific retinal pigmentation results in sexually dimorphic long-wavelength-sensitive photoreceptors in the eastern pale clouded yellow butterfly, *Colias erate*. *The Journal of Experimental Biology*, *216*, 1916–1923.

Oksanen, J., Blanchet, F. G., Friendly, M., Kindt, R., Legendre, P., McGlinn, D., Minchin, P. R., O'Hara, R. B., Simpson, G. L., Solymos, P., Stevens, M. H. H., Szoecs, E., & Wagner, H. (2019). *Vegan: Community ecology package*. R Package Version 2.5-5. https://CRAN.R-project.org/package=vegan

Papke, R. S., Kemp, D. J., & Rutowski, R. L. (2007). Multimodal signalling: Structural ultraviolet reflectance predicts male mating success better than pheromones in the butterfly *Colias eurytheme* L. (Pieridae). *Animal Behaviour*, *73*, 47–54.

Paris, J. R., Stevens, J. R., Catchen, J. M., & Johnston, S. (2017). Lost in parameter space: A road map for stacks. *Methods in Ecology and Evolution*, *8*, 1360–1373.

Pérez i de Lanuza, G., Font, E., & Carazo, P. (2013). Color-assortative mating in a color-polymorphic lacertid lizard. *Behavioral Ecology*, *24*, 273–279.

Peterson, B. K., Weber, J. N., Kay, E. H., Fisher, H. S., & Hoekstra, H. E. (2012). Double digest RADseq: An inexpensive method for de novo SNP discovery and genotyping in model and non-model species. *PLoS One*, *7*, e37135.

Pfennig, D. W., Wund, M. A., Snell-Rood, E. C., Cruickshank, T., Schlichting, C. D., & Moczek, A. P. (2010). Phenotypic plasticity's impacts on diversification and speciation. *Trends in Ecology & Evolution*, *25*, 459–467.

Pigliucci, M., & Preston, K. (2004). *Phenotypic integration: Studying the ecology and evolution of complex phenotypes*. Oxford University Press.

Polic, D., Yıldırım, Y., Lee, K. M., Franzén, M., Mutanen, M., Vila, R., & Forsman, A. (2022). *Linking large-scale genetic structure of three Argynnini butterfly species to geography and environment*. NCBI SRA, BioProject ID PRJNA70744.

Polic, D., Yıldırım, Y., Merilaita, S., Franzén, M., & Forsman, A. (2022). *Genetic structure, UV-vision, wing coloration and size coincide with colour polymorphism in Fabriciana adippe butterflies*. NCBI SRA, BioProject ID PRJNA838593.

Polic, D., Yıldırım, Y., Vila, R., Ribeiro Cardoso, P. R., Franzén, M., & Forsman, A. (2023). Large-scale spatial variation and phenotypic integration in three *Argynnini* species inform about functions and evolutionary drivers of butterfly wings. *Frontiers in Ecology and Evolution*, *11*, 1087859.

Priyam, A., Woodcroft, B. J., Rai, V., Moghul, I., Munagala, A., Ter, F., Chowdhary, H., Pieniak, I., Maynard, L. J., & Gibbins, M. A. (2019). Sequenceserver: A modern graphical user interface for custom BLAST databases. *Molecular Biology and Evolution*, *36*, 2922–2924.

R Core Team. (2020). *R: A language and environment for statistical computing*. R Foundation for Statistical Computing. https://www.R-project.org/

Rankin, K., & Stuart-Fox, D. (2015). Testosterone-induced expression of male colour morphs in females of the polymorphic tawny dragon lizard, *Ctenophorus ddecresii*. *PLoS One*, *10*, e0140458.

Rankin, K. J., McLean, C. A., Kemp, D. J., & Stuart-Fox, D. (2016). The genetic basis of discrete and quantitative colour variation in the polymorphic lizard, *Ctenophorus ddecresii*. *BMC Evolutionary Biology*, *16*, 179.

Rodnina, M. V. (2013). The ribosome as a versatile catalyst: Reactions at the peptidyl transferase center. *Current Opinion in Structural Biology*, *23*, 595–602.

Roulin, A. (2004). The evolution, maintenance and adaptive function of genetic colour polymorphism in birds. *Biological Reviews*, *79*, 815–848.

Rousset, F., & Raymond, M. (1995). Testing heterozygote excess and deficiency. *Genetics*, *140*, 1413–1419.

Russo, C. A. M., Solé-Cava, A. M., & Thorpe, J. P. (1994). Population structure and genetic variation in two tropical sea anemones (Cnidaria, Actinidae) with different reproductive strategies. *Marine Biology*, *119*, 267–276.

Ruxton, G. D., Sherratt, T. N., & Speed, M. P. (2004). *Avoiding attack: The evolutionary ecology of crypsis, warning signals and mimicry*. Oxford University Press.

San-Jose, L. M., & Fitze, P. S. (2013). Corticosterone regulates multiple colour traits in Lacerta [Zootoca] vivipara males. *Journal of Evolutionary Biology*, *26*, 2681–2690.

Sapir, Y., Gallagher, M. K., & Senden, E. (2021). What maintains flower colour variation within populations? *Trends in Ecology & Evolution*, *36*, 507–519.

Schlichting, C. D., & Wund, M. A. (2014). Phenotypic plasticity and epigenetic marking: An assessment of evidence for genetic Accommodation. *Evolution*, *68*, 656–672.

Schwander, T., & Leimar, O. (2011). Genes as leaders and followers in evolution. *Trends in Ecology & Evolution*, *26*, 143–151.

Schweiger, A. H., & Beierkuhnlein, C. (2016). Size dependency in colour patterns of Western palearctic carabids. *Ecography*, *39*, 846–857.

Shakya, S. B., Haryoko, T., Irham, M., Suparno, Prawiradilaga, D. M., & Sheldon, F. H. (2021). Genomic investigation of colour polymorphism and phylogeographic variation among populations of black-headed bulbul (*Brachypodius atriceps*) in insular southeast Asia. *Molecular Ecology*, *30*, 4757–4770.

Sharkia, R., Jain, S., Mahajnah, M., Habib, C., Azem, A., Al-Shareef, W., & Zalan, A. (2023). PTRH2 gene variants: Recent review of the phenotypic features and their bioinformatics analysis. *Genes*, *14*, 1031.

Shine, R., Brown, G. P., & Phillips, B. L. (2011). An evolutionary process that assembles phenotypes through space rather than through time. *Proceedings of the National Academy of Sciences of the United States of America*, *108*, 5708–5711.

Silberglied, R. E. (1984). Visual communication and sexual selection among butterflies. In R. I. Vane-Wright & P. R. Ackery (Eds.), *The biology of butterflies* (pp. 207–223). Academic Press.

Skórka, P., Nowicki, P., Kudłek, J., Pępkowska, A., Śliwińska, E., Witek, M., Settele, J., & Woyciechowski, M. (2013). Movements and flight morphology in the endangered large blue butterflies. *Open Life Sciences*, *8*, 662–669.

Stella, D., Pecháček, P., Meyer-Rochow, V. B., & Kleisner, K. (2018). UV reflectance is associated with environmental conditions in Palaearctic *Pieris napi* (Lepidoptera: Pieridae). *Insect Science*, *25*, 508–518.

Stuart-Fox, D., Aulsebrook, A., Rankin, K. J., Dong, C. M., & McLean, C. A. (2021). Convergence and divergence in lizard colour polymorphisms. *Biological Reviews*, *96*, 289–309.

Stuhldreher, G., Hermann, G., & Fartmann, T. (2014). Cold-adapted species in a warming world – An explorative study on the impact of high winter temperatures on a continental butterfly. *Entomologia Experimentalis et Applicata*, *151*, 270–279.

Svensson, E. I., Arnold, S. J., Bürger, R., Csilléry, K., Draghi, J., Henshaw, J. M., Jones, A. G., De Lisle, S., Marques, D. A., McGuigan, K., Simon, M. N., & Runemark, A. (2021). Correlational selection in the age of genomics. *Nature Ecology & Evolution*, *5*, 562–573.

Takahashi, T., & Hori, M. (2008). Evidence of disassortative mating in a Tanganyikan cichlid fish and its role in the maintenance of intrapopulation dimorphism. *Biology Letters*, *4*, 497–499.

Tamin, T., & Doligez, B. (2022). Assortative mating for between-patch dispersal status in a wild bird population: Exploring the role of direct and indirect underlying mechanisms. *Journal of Evolutionary Biology*, *35*, 561–574.

Thompson, M. J., & Jiggins, C. D. (2014). Supergenes and their role in evolution. *Heredity*, *113*, 1–8.

Tolman, T., & Lewington, R. (2012). *Schmetterlinge Europas und Nordwestafrikas* (2nd ed.). Franckh-Kosmos Verlag.

True, J. R. (2003). Insect melanism: The molecules matter. *Trends in Ecology & Evolution*, *18*, 640–647.

Tsai, C.-C., Childers, R. A., Nan Shi, N., Ren, C., Pelaez, J. N., Bernard, G. D., Pierce, N. E., & Yu, N. (2020). Physical and behavioral adaptations to prevent overheating of the living wings of butterflies. *Nature Communications*, *11*, 551.

Van Belleghem, S. M., De Wolf, K., & Hendrickx, F. (2016). Behavioral adaptations imply a direct link between ecological specialization and reproductive isolation in a sympatrically diverging ground beetle. *Evolution*, *70*, 1904–1912.

VanKuren, N. W., Doellman, M. M., Sheikh, S. I., Droguett, D. H. P., Massardo, D., & Kronforst, M. R. (2022). Conserved signaling pathways antagonize and synergize with co-opted *doublesex* to control development of novel mimetic butterfly wing patterns. *bioRxiv*. https://doi.org/10.1101/2022.09.20.508752

Villamor, A., Signorini, L. F., Costantini, F., Terzin, M., & Abbiati, M. (2020). Evidence of genetic isolation between two Mediterranean morphotypes of *Parazoanthus axinellae*. *Scientific Reports*, *10*, 13938.

Vukusic, P., & Sambles, J. R. (2003). Photonic structures in biology. *Nature*, *424*, 852–855.

Wang, I. J., & Summers, K. (2010). Genetic structure is correlated with phenotypic divergence rather than geographic isolation in the highly polymorphic strawberry poison-dart frog. *Molecular Ecology*, *19*, 447–458.

Warren, M. S. (1995). Managing local microclimates for the high brown fritillary, *Argynnis adippe*. In A. S. Pullin (Ed.), *Ecology and conservation of butterflies* (pp. 198–210). Springer Netherlands.

Weir, B. S., & Cockerham, C. C. (1984). Estimating F-statistics for the analysis of population structure. *Evolution*, *38*, 1358–1370.

Wellenreuther, M., Svensson, E. I., & Hansson, B. (2014). Sexual selection and genetic colour polymorphisms in animals. *Molecular Ecology*, *23*, 5398–5414.

Wennersten, L., & Forsman, A. (2012). Population-level consequences of polymorphism, plasticity and randomized phenotype switching: A review of predictions. *Biological Reviews*, *87*, 756–767.

Werren, J. H., Baldo, L., & Clark, M. E. (2008). Wolbachia: Master manipulators of invertebrate biology. *Nature Reviews Microbiology*, *6*, 741–751.

Westerman, E. L., Chirathivat, N., Schyling, E., & Monteiro, A. (2014). Mate preference for a phenotypically plastic trait is learned, and may facilitate preference-phenotype matching. *Evolution*, *68*, 1661–1670.

Westerman, E. L., Letchinger, R., Tenger-Trolander, A., Massardo, D., Palmer, D., & Kronforst, M. R. (2018). Does male preference play a role in maintaining female limited polymorphism in a Batesian mimetic butterfly? *Behavioural Processes*, *150*, 47–58.

Westerman, E. L., VanKuren, N. W., Massardo, D., Tenger-Trolander, A., Zhang, W., Hill, R. I., Perry, M., Bayala, E., Barr, K., & Chamberlain, N. (2018). Aristaless controls butterfly wing color variation used in mimicry and mate choice. *Current Biology*, *28*, 3469–3474.

Whitman, D. W., & Agrawal, A. A. (2009). What is phenotypic plasticity and why is it important. In D. Whitman (Ed.), *Phenotypic plasticity of insects: Mechanisms and consequences* (pp. 1–63). CRC Press.

Whitney, J. L., Bowen, B. W., & Karl, S. A. (2018). Flickers of speciation: Sympatric colour morphs of the arc-eye hawkfish, *Paracirrhites arcatus*, reveal key elements of divergence with gene flow. *Molecular Ecology*, *27*, 1479–1493.

Willing, E.-M., Dreyer, C., & van Oosterhout, C. (2012). Estimates of genetic differentiation measured by FST do not necessarily require large sample sizes when using many SNP markers. *PLoS One*, *7*, e42649.

Wilts, B. D., Pirih, P., Arikawa, K., & Stavenga, D. G. (2013). Shiny wing scales cause spec(tac)ular camouflage of the angled sunbeam butterfly, *Curetis acuta*. *Biological Journal of the Linnean Society*, *109*, 279–289.

Winter, G., Varma, M., & Schielzeth, H. (2021). Simple inheritance of color and pattern polymorphism in the steppe grasshopper *Chorthippus dorsatus*. *Heredity*, *127*, 66–78.

Wright, S. (1984). *Evolution and the genetics of populations, volume 3: Experimental results and evolutionary deductions*. University of Chicago press.

Yildirim, Y., Tinnert, J., & Forsman, A. (2018). Contrasting patterns of neutral and funtional genetic diversity in stable and disturbed environments. *Ecology and Evolution*, *8*, 12073–12089.

SUPPORTING INFORMATION

Additional supporting information can be found online in the Supporting Information section at the end of this article.

How to cite this article: Polic, D., Yıldırım, Y., Merilaita, S., Franzén, M., & Forsman, A. (2024). Genetic structure, UV-vision, wing coloration and size coincide with colour polymorphism in *Fabriciana adippe* butterflies. *Molecular Ecology*, *00*, e17272. https://doi.org/10.1111/mec.17272